Report R-217

DESIGN OF LOW-POWER PULSE TRANSFORMERS USING FERRITE CORES

by
Richard Dwight Robinson

FOREWORD

The recently developed group of magnetic ferrite materials present attractive possibilities for use in the cores of transformers designed to handle low-power short-duration voltage or current pulses. Because these materials possess high resistivity, the effect of eddy currents at high frequencies is reduced. They may be used at higher effective permeabilities than metals. Thus transformers with ferrite cores can be physically very small, an important consideration in applications such as digital computers where large numbers of transformers are required.

Because this thesis report, which has had only limited distribution, contains information on this subject of widespread interest, it is being issued as a Digital Computer Laboratory R-series report.

The author is indebted to the staff and personnel of the M.I.T. Digital Computer Laboratory under the directorship of Mr. Jay W. Forrester for presenting the thesis problem and assisting in this research. Special acknowledgments are made to Mr. Robert E. Hunt of the Digital Computer Laboratory for developing the fabrication technique of the pulse transformers and to Mr. David J. Epstein of the Laboratory for Insulation Research for conducting the d-c pulse tests on the ferrite materials.

ABSTRACT

This report presents the design procedure for constructing pulse transformers of ferrite materials for Whirlwind I Digital Computer to replace those made of Hypersil. The ferrite materials are ceramic-type materials with the unusual combination of properties of ferromagnetism and high electrical resistivity. The high resistivity reduces the effect of eddy currents at high frequencies so that higher effective permeabilities are observed than with metallic materials.

Effective pulse permeabilities of those ferrites tested range up to a maximum of 450 for 0.1-microsecond pulses, while that observed for 1-mil Hypersil (with air gap) is approximately 100.

Equivalent circuits for the 3:1 and the 1:1 pulse transformers in WWI when made from ferrite materials are developed. An analytical determination of output waveshape is made using these simple equivalent circuits and shown to be in close accord with the observed experimental results.

The assembly and circuit test of 1-to-1 and 3-to-1 ferrite transformers for use in Whirlwind I circuits are discussed. The transformers described are equivalent in performance to the Hypersil transformer now used, and yet are more simply constructed and more compact, and can be produced at considerably lower cost. Ferrite-core pulse transformers are admirably suited for 0.1-microsecond pulse applications.

Report R-217

TABLE OF CONTENTS

LIST OF ILLUSTRATIONS

CHAPTER I

INTRODUCTION

A pulse transformer as defined by common usage is a transformer designed specifically for handling voltage or current pulses with time durations in the order of micro- or millimicro-seconds. Because these transformers perform only under high frequency excitations, the number of turns required to produce a given voltage is small, and for low-power applications the physical size of a pulse transformer can be made correspondingly small. These transformers are common in radar and television circuitry, and in Whirlwind I (WWI) computer over 3,000 pulse transformers are used for coupling between circuits where they permit a saving in the number and size of tubes required.

The most common pulse shape which a pulse transformer in WWI is required to handle is a half-sine shape of 0.1 microsecond pulse duration, occurring at pulse repetition frequencies of from 1 to 2 mc. The two most common voltage ratios are 3:1 and 1:1, the former being used for mixing and remote point-to-point coupling, while the latter is used for local point-to-point coupling. For these applications Hypersil core transformers were designed by Wimett[1] and have been in successful operation for several years.

The introduction of the new ferromagnetic ceramic materials or "ferrites" on the market have caused several component manufacturers to introduce pulse transformers incorporating this material with resulting smaller physical dimensions and lighter weight. A few samples of these ferrite transformers were tested at Whirlwind, but found unsatisfactory. It was

---

1. Wimett, T. E., "Low Power Pulse Transformers," Report R-122, Servomechanisms Laboratory, M. I. T., December, 1947.

then decided that a research into pulse transformer design for Whirlwind I

using the ferrite core materials was warranted. This research would have

the following objectives:

(a) To determine the properties of those ferrites commercially

available as related to pulse transformer application.

(b) To formulate a design technique for ferrite pulse transformers

which would give the particular performance required in WWI circuitry.

(c) To develop equivalent circuit of the completed pulse trans-

former.

(d) To compare the cost, performance and physical dimensions of

a ferrite core pulse transformer with the Hypersil transformers currently in

use in WWI.

There were two reasons for the first objective of determining the

properties of ferrites. First, the manufacturers of these materials in

most cases have published only d-c hysteresis loops and resitivity data.

Second, in designing pulse transformers using metallic cores it was necessary

to make assumptions concerning the magnetic state of the material due to the

extreme eddy-current shielding effects. Hence the core requirements were

stated only in great generalities, although attempts were made to define a

"pulse permeability."[2] The high resistivities of the ferrites however give

promise of reducing the eddy-current shielding to such a low degree that

correlation of d-c data and pulse response can be made. Such correlation

was obtained in this research and will be pointed out in this report.

The second objective, that of formulating a design technique,

necessarily follows the introduction of any radically different material

---

2. Moody, N. F., "A Treatise on the Design of Pulse Transformers For
   Handling Small Powers," TRE 4310.

in a component. For example, it will be shown that in the WWI 1:1 pulse
transformer a certain amount of leakage inductance is actually necessary
for the desired performance. In the Hypersil design, this leakage was
readily available, but in a ferrite design it was necessary to introduce
it by separating the windings.

One of the most useful tools of the electrical circuit designer
is the equivalent circuit. In the case of metallic-core pulse transformers
an elaborate equivalent circuit has often become so complicated as to lose
its value as an aid to the designer. The third ojbective then was to develop
a simple equivalent circuit which could be used to predict performance.
Finding an equivalent circuit was successfully done in this thesis for two
very important reasons. First, the ferrite material by permitting a reduction
in number of turns and in plysical size caused a corresponding reduction in
distributed capacitance and leakage inductance to a point where they no
longer became major parameters. Second, the shape of the pulse being con-
sidered was not a square wave but a half-sine shape. For those who like to
think in terms of frequency response, the second consideration reduces the
pass-band requirements of the transformer, thus reducing the noticeable
effect of stray capacities.

The fourth and final objective of this research was to evaluate
the completed design. This is done in the final section of the thesis and
it should be noted that the new ferrites find excellent application in pulse
transformers.

In the organization of this thesis report, the order of presentation
is similar to the research objectives outlined above. In Chapter II, the
investigations into the magnetic properties of some ferrites are described,
and the resulting data analyzed to give criteria for optimum pulse trans-
former performance. In Chapter III, the design of a 3:1 and a 1:1 pulse

transformer using the material properties of Chapter II are described.
Before the actual design procedure is introduced, however, the equivalent
circuit is presented and an analytical determination of wave-shape response
made. Chapter IV describes the construction and test performance of the
designs given in Chapter III. Finally, in Chapter V the thesis report is
summarized.

It should be noted that the design procedures followed in this
thesis are for half-sine pulse shapes rather than the customary square wave.
The analysis and design of pulse transformers for square-wave response are
fairly well developed in several texts and reports[3] and the reader is
referred to these sources for the typical procedure. If, however, the
square-wave design procedures are followed for other pulse shapes, such as
the half-sine, one is faced with the problem of correlating the two per-
formances. It is not sufficient to say that a pulse transformer which will
pass a square wave will pass any wave shape. For while this is true with
regard to the positive-going portion of the pulse, one may, for example,
desire a high over-shoot and fast decay on the negative-going portion of
the pulse. Or as another example, the transformer may be required to "ring"
when driven by a half-sine pulse. To correlate these required performances
with square-wave response is difficult if the driving function is not a
square wave itself. For this reason, the design procedure presented here
is for the particular case of a half-sine driving function.

Chapter II on ferrite core magnetic characteristics is, however,
applicable to any driving function design. Thus the values of pulse

---

3. For example: Wimett (Ref. 1), Moody (Ref. 2) and Glasoe and Lebacqz,
   Pulse Generators, McGraw-Hill Book Co., Inc. Rad. Lab. Series No. 5,
   pp. 499-660; or Lee, R., Electronic Transformers and Circuits, John
   Wiley & Sons, Inc., New York, 1947.

permeability which were experimentally determined may be used for any pulse transformer design where the pulse width is in the order of 0.1 microseconds or greater.

CHAPTER II

MAGNETIC TESTING OF FERRITES

A variety of ferrite materials in the form of small toroids with dimensions 3/8" outside diameter, 3/16" inside diameter, and 1/8" thick were obtained from several ferrite manufacturers. These materials were then given symmetrical 60-cycle tests and high-and low-speed non-symetrical pulse loop tests.

A. 60-CYCLE TEST

The main purpose of this test was to establish the general shape of the low speed magnetization curve. For this purpose, the 60-cycle hysteresis-loop tracer in the Digital Computer Laboratory was used, this equipment having been constructed especially for the testing of small ferrite cores. These curves were then checked with d-c hysteresis loops taken on the Cioffi-type Hysteresograph in the Laboratory for Insulation Research at M. I. T. and the two methods were found to give identical shape traces.

B. PULSE TESTS

In order to perform high-speed pulse tests it was necessary to construct some special equipment. This equipment which is shown in Figure 1 and which is discussed in detail in Appendix A consisted of a gas-tube pulse generator capable of producing half-sine pulses of current with time durations of from 0.1 to 0.3 microseconds and with peak amplitudes up to 1 ampere. The specimen to be tested was wound with 10 turns and placed in the cathode circuit of the generator. The standard procedure followed was to integrate the voltage across the windings to measure flux density B and to read the voltage across a small series resistor to measure magnetizing force H. This apparatus permitted the visual indication of a pulse hysteresis loop under conditions similar to those existing when the material is used as a pulse transformer.

The presence of the Cioffi-type Hysteresograph at M. I. T. afforded the opportunity to draw slow-time-pulse hysteresis loops for comparison with the high-speed loops obtained from the gas-tube pulse generator. For this test two concentric windings of 25 turns each were wound on the specimen. The slow-time or "d-c pulse loops" were taken by starting with the material in a virgin magnetic state and applying a series of slowly varying unidirectional current excitations of constant peak amplitude. Following the procedure used in the high-speed pulse test, the peak amplitude was then reduced without cycling the material back to the initial virgin state and another d-c pulse loop drawn. This was repeated for several values of peak excitation.*

C. ANALYSIS OF PULSE LOOPS

The formation of a pulse hysteresis loop using the gas-tube pulse generator is shown in Figure 2. Because the technique of photographing the oscilloscope picture results in the time trace going from right to left, the sketches were also drawn in this manner. Referring to Figure 2 it is seen that with R_1 small, v_1 represents the excitation current and v_2 is the integral of v_t, which is substantially the voltage across the winding of the sample. The oscilloscope traces for each of these voltages are sketched in the figure as well as the formation of a pulse loop when v_1 is applied to the horizontal deflection plates and v_2 to the vertical deflection plates of an oscilloscope. It will be noted that following the completion of the current pulse, the total voltage across the winding v_t does not return immediately to zero, a fact which is better illustrated by the slow decay of v_2, the time integral of v_t. These sketches represent the observed results and will be discussed next in conjunction with the formation of the slow time or d-c

---

* These d-c pulse tests were conducted by Mr. D. J. Epstein of the Laboratory for Insulation Research, M. I. T.

pulse loop.

Figure 3, "The Formation of a D-C Pulse Loop," is an actual trace

of the pulse response of Ferramic H* taken on the Cioffi-type Hysteresograph.

From the initial virgin condition the loci is seen to traverse to a B_{max} point

and then return to the residual induction point B_r. Succeeding pulses of the

same maximum H amplitude then trace a pulse loop between B_{max} and B_r. In

this kind of a slow trace, there is no problem of the material not respond-

ing immediately to the current forcing function H. If the speed of the applied

H were to be increased, however, a material with a low electrical resistivity

would have large induced eddy currents. These eddy currents would effectively

"screen" much of the center portion of the test sample so that the outside

surface would approach saturation while the inner portion remained relatively

undisturbed magnetically. If the same value of cross-sectional areas were

used for computing flux density B for the high-speed pulse traces as for the

slow-speed traces, then for the same amplitude of H there would be no similarity

in the values of the total ΔB observed, $(\Delta B = B_{max} - B_r)$.

In the high resistivity ferrites on the other hand, for the same

maximum applied H almost the same ΔB was observed for the 0.1 microsecond

pulse as for the d-c pulse. This indicates that eddy currents are practically

negligible in these materials for frequencies up to 5 megacycles, the frequency

corresponding to the half-sine pulse of width 0.1 microseconds.

In the high-speed pulse loops for the ferrites it was observed that

while the end points B_{max} and B_r were the same as those for the d-c pulse

loop, the actual return path from B_{max} departed from that of the d-c pulse

loop. This is shown in Figure 3 where the 0.1 microsecond pulse loop strikes

---

* The trade name of a ferrite produced by General Ceramics and Steatite
  Corporation.

a point B_r' on the B-axis and then returns to B_r. From experiments it was

found that as the maximum applied H was increased in the fast-time pulse

tests so that the material was driven further and further into saturation,

the value of $B_r' - B_r$ became a larger proportion of $B_{max} - B_r$. In fact,

for the 0.1 microsecond pulses it appears to be a good approximation to

say that the return route from B_{max} is along a straight line which has the

same slope as the initial slope of the d-c return path.

The rate of time decay of the fast-time pulse loops from B_r' to B_r

was found to vary, depending upon the nature of the material under test.

One material, MF-1131,* which has a rectangular d-c hysteresis loop ferrite,

has an extremely long decay rate as compared to the other ferrites with non-

rectangular d-c hysteresis loops. No explanation is given here for the factors

affecting this rate of decay other than to say that investigations were made

to assure that leakage capacitances, number of turns, and integration time

constants were not causing this phenomenon.

D. DATA SUMMARY

Figure 4 shows some typical 60-cycle hysteresis loops of the ferrites

tested. It will be noted that there is available a fairly wide choice in the

d-c magnetic characteristics.

Figures 5 and 6 show pulse hysteresis loops taken of several

materials at pulse lengths ranging from 0.1 to 0.3 microseconds. The values

of ΔB_{max} and ΔH_{max} for the largest pulse loop is given under the figure.

The voltage shapes below the pulse loops are in the same order of presentation

as those sketched in the top right portion of Figure 2.

The pulse magnetization response of various ferrites is presented

---

* A General Ceramics and Steatite Corporation material.

in Figure 7 in the form of a plot of $\triangle$B vs. $\triangle$H. These curves are loci of
the tips of the high-speed pulse loops for various values of applied $\triangle$H.
Included is a test result on 1-mil Hypersil. In computing the value of $\triangle$B
for Hypersil, the cross sectional area used does not include a lamination
space factor, so that the $\triangle$B values are slightly low.

Both the Hypersil and the Ferroxcube 3C samples have air gaps,
these being the only samples readily available for this research. The effect
of the air gap on a magnetic material is to shear the d-c magnetization curve.[4]
This causes the residual induction B_r to become less and permits a greater
range of pulse operation before saturation is reached. By the proper amount
of shear it is also possible in some materials to realize a slightly greater
"effective pulse permeability", μ_e, which is here defined as $\triangle$B/$\triangle$H. The
reason for this is that in shearing the hysteresis loop the pulse operation
is further away from the saturation regions and hence in the higher a-c
permeability regions.

Figure 8 shows the correlation between fast-time and d-c pulse
response for Ferramic H. In this figure, the end-points $\triangle B_{max}$, $\triangle H_{max}$, are
plotted for different values of pulse loop amplitudes. This shows that
within the limits of experimental error there is no difference in the end
points of pulse loops for Ferramic H from pulse speeds of "d-c" to 0.1
microsecond. (B_r' is not concerned in this plot.)

Figure 9 shows the correlation between d-c pulse and 0.1 microsecond
pulse response for various materials. Note the great discrepancy in the data
on Hypersil.

The significance of these test results is that for pulse lengths
at least as short as 0.1 microsecond the d-c magnetization curve may be used

---

4. M. I. T. Staff, Magnetic Circuits and Transformers, pp. 65-68, John Wiley
   & Sons, 1943.

to predict the performance of the high-resistivity ferrites to pulse excita-
tions. This may be done by considering the material is initially at the
residual induction value B_r of Figure 3 (as it certainly will be after the
first pulse). Then a d-c pulse loop of the general shape shown in Figure 3
may be sketched. The resulting line from B_r out to B_{max} may then serve as
loci for $\triangle B$ and $\triangle H$ values for use in fast pulse calculations.

Table 1 summarizes the data for the materials tested, and includes
the information that was available from the manufacturers. The discrepancy
in the values of B_{max} between the Test Data and the Manufacturer's Data is
due to the difference in applied H_{max} for the two cases.

E. EVALUATION OF FERRITES FOR PULSE TRANSFORMERS

From Table 1 it can be seen that the effective pulse permeabilities
of those ferrites tested range up to a maximum of 450. For 0.1 microsecond
pulses this is a much better value than for grain-oriented steels. Moody[2]
gives values of 130 for 3-mil Hypersil and 210 for 4-mil Mumetal at this pulse
length. For 1 microsecond pulses these values increase to 400 and 720 respec-
tively. Thus on the basis of pulse permeability alone, it is seen that the
ferrite is a superior material for pulse lengths shorter than about 0.5 micro-
seconds.

The ferrites lose some of their advantage by having relatively low
saturation inductions. This means that if the material is used for long pulses
or for high voltages then the core area must be increased sufficiently to
prevent the material from going into saturation. As was mentioned earlier it
is advantageous to introduce an air gap in these cases to permit higher values
of permissible $\triangle B$.

Another disadvantage of the ferrites is their low Curie temperature,
i.e. - the temperature at which the material loses its magnetic properties.
This may be serious if the transformer is to be mounted near a source of heat,

2. Ibid.

and the designer may well keep this in mind when laying out his circuit.

For the application in Whirlwind I, none of these disadvantages are particularly important. The 3:1 and 1:1 pulse transformers are low-power devices and operate under 0.1 microsecond pulse excitations. Further-more, there is no particular problem of heat dissipation since the circuits are well laid out for ventilation. Thus, from the standpoint of the magnetic properties the ferrites would appear to fit this application well. The next chapter will deal with the problem of designing the 3:1 and 1:1 ferrite-core pulse transformers for WWI.

			Manufacturers' Data			Test Data (at H_{max} = 7 oersteds)				
Material	ρ(ohm-cm)	Curie Temp.	Maximum Values			B_r Gauss	H_c Oersteds	B_{max} Gauss	ΔB_{max}	μ_e average effective pulse permeability
			B_r Gauss	H_c Oersteds	B_{max} Gauss					
Ceramag 7A	3×10^5	$165^\circ C$	3600	0.6	4160	1100	0.18	2380	1280	350
Ceramag 5N						1150	0.45	2510	1360	380
Ferramic H	1×10^4	$150^\circ C$	1470	0.18	3400	1600	0.18	2320	720	450
Ferroxcube 3C (with air gap)	1×10^2	$160^\circ C$	1200	0.2	3500					450
Ferricore						950	1.06	2300	1350	230
MF-1131						1900	1.03	2300	400	40

Material	Manufacturer
Ceramag 7A	Stackpole Carbon Company
Ceramag 5N	" " "
Ferramic H	General Ceramics & Steatite Corp.
MF-1131	" " " " "
Ferroxcube 3C	Ferroxcube Corp. of America
Ferricore	Ferricore Company

TABLE I

SUMMARY OF MAGNETIC DATA ON FERRITES

CHAPTER III

PULSE TRANSFORMER DESIGN

A. INTRODUCTION

In designing pulse transformers for WWI circuitry, there are several objectives that the designer must keep in mind. As an example, for the 3:1 pulse transformer which operates under 0.1 microsecond half-sine excitation, these objectives include wave shape preservation of the positive portion of the pulse and rapid recovery of the overshoot. Before the design can be attempted then, the designer must understand the effects of the various transformer parameters on the output wave shape. These parameters, which include mutual inductance, leakage inductance, distributed capacitance and an equivalent loss resistance, will assume various degrees of importance in shaping the output waveform. Furthermore, the kind of loading and the nature of the driving source will also influence the final shape of the transformed pulse, so that it is necessary to consider the entire circuit in which the transformer is to operate in the design procedure.

For these reasons, a considerable portion of this chapter is spent on showing the distortions produced by the different circuit parameters. To develop this "feeling" for the parameter effects, a "Basic Transformer" is first introduced which has neither leakage inductance nor distributed capacitance. The magnetizing current and the output voltage shapes of such a transformer are described when driven by a half-sine pulse current source for the conditions of no-load and of large load. Constant reference is made to the B-H plane in order to relate the magnetic state of the core material to output wave shape.

Following these concepts of the Basic Transformer, the equivalent circuit for a 3:1 pulse transformer to be used in WWI applications is presented.

The analytical determination of output voltage wave shape is carried out and
the design procedure described. This in turn is followed by the equivalent
circuit and design procedure for a 1:1 pulse transformer when operated under
no-load conditions, this being the condition of operation in WWI of the 1:1
transformer.

B. BASIC PULSE TRANSFORMER WAVE SHAPES

The pulse loops of Figures 5 and 6 were taken with a half-sine
wave of current excitation. This is essentially the condition of a pulse
transformer under open-circuit conditions when driven by a current source such
as a pentode in Class B operation with a half-sine wave impressed upon the
grid. Neglecting the practical considerations of leakage flux, stray and
winding capacitances, the transformer would produce across its output terminals
a symetrical cosine voltage shape as illustrated in the portion of Figure 10
where a constant permeability μ is assumed.

If, however, the permeability were to change at the peak of the
magnetizing current wave form μ to some smaller value μ', then the negative
peak of the voltage wave v_t would have a smaller absolute magnitude than the
positive peak. Assuming a quasi-steady state condition, after time T the
material must return from B_r' to its inital starting point B_r. Since

$$\int_{t=0}^{t=T/2} v_t \, dt = N\int_{\phi_1}^{\phi_2} d\phi = -\int_{t=T/2}^{t\rightarrow\infty} v_t \, dt$$

the areas under the positive and negative portions of the voltage plot must
be equal, or the integral $v_2 = \int v_t \, dt$ must go to zero. This decay of v_2
was described in the preceeding chapter as dependent upon an intrinsic lag
of the material.

Next consider the effect of placing a load resistor across the
transformer terminals as in Figure 11. If R is sufficiently small so that
the magnetizing current through the transformer is but a fraction of the
current through R, the half-sine current source may be replaced with a half-
sine voltage source with series resistance R. The current i_m in this equiva-
lent circuit is the magnetizing current through the basic transformer.

Because i_m is proportional to the integral of v_t it will be
approximately a cosine-shape wave from time $t = 0$ to $t = T$. It is interesting
to note that from $t = 0$ to $t = T$ i_m is always increasing so that the pulse
hysteresis loop is now traversed from $B_r \rightarrow B_{max}$ in twice the time as with
the open-circuited transformer. With the material in a magnetic state of
H_{max}, B_{max} the voltage source is shorted and the transformer is left with the
load resistor R across its terminals. Since the magnetizing current is still
finite, it continues to flow and causes a reverse peak on v_t of magnitude $I_m R$.
For the case of constant permeability, the reverse voltage of v_t then goes to
zero with an exponential decay of time constant L/R. That this satisfies the
condition of equal areas under the positive and negative portions of the v_t wave
can be shown by letting the voltage v_t be a true half-sine wave from $t = 0$ to
$t = T$. Then

For $0 \leq t \leq T$

$$e_t = E \sin \omega t$$

at $t = T$,

$$i_m = I_m = \int_0^{\pi} \frac{E}{\omega L} \sin \omega t \, d(\omega t) = 2E/\omega L$$

$$\int_0^{\pi} e_t \, dt = 2E/\omega$$

For $t > T$

$$e_t' = - I_m R e^{-Rt/L}$$

as $t \rightarrow \infty$

$$\int_o^{\infty} e_t' \, dt = \frac{-2ER}{\omega L} \int_0^{\infty} e^{-Rt/L} \, dt$$

$$= - 2E/\omega$$

Thus the areas are equal.

If the case of a change in permeability is considered as in

Figure 11, then the shape of the decay of the negative overshoot in v_t will

no longer be a single exponential curve. In terms of the pulse loops of

Figure 3, for R very small the d-c pulse return path will be followed. As

R increases, the loci will approach that of the open-circuited case discussed

previously. In any case, the initial slope of the returning loci will be

that of the d-c return path. In Figure 11, the change in permeability is

pictured in distinct steps which result in the three permeability values

μ, μ', and μ''. The effects of μ' and μ'' on the voltage overshoot are to

give a two different time constant exponential decay. Compared with the con-

stant μ case, the overshoot will at first decay more rapidly, and then at

time T' will follow a very much slower rate of decay. Again, however, the

areas of the positive and negative portions of the v_t curve must be equal.

From this consideration of the effect of load on the output wave

shape of the basic transformer, the next section describes the 3:1 pulse

transformer equivalent circuit and its analysis.

C. THE 3:1 PULSE TRANSFORMER EQUIVALENT CIRCUIT

A standard equivalent circuit which is generally drawn for a pulse

transformer is the general equivalent circuit of Figure 12. In this circuit,

all elements are referred to the primary. Here R_1 and R_2 represent winding

resistances of the primary and secondary windings, R_e represents the trans-

former losses, ℓ_1 and ℓ_2 the leakage inductances, L the primary self in-

ductance or "open circuit" inductance, C_m the winding-to-winding capacitance,

and C_p and C_s include the distributed capacitance of the windings as a lumped

parameter along with the external stray, source, and load capacitances.

Because this circuit is too complicated for analysis, it is common

practice to neglect those parameters which produce second-order effects and

to resort to a reduced equivalent circuit. The leakage inductance ℓ_1 and

$a^2 \ell_2$ are lumped into a single element ℓ, the winding resistances are neglected, and the effects of C_m combined with C_p when the voltage ratio a is greater than 1, or with C_s if a is less than 1. The equivalent trans-former loss resistor R_e is also omitted.

In measurements taken on the 3:1 pulse transformers designed in this research, it was found that the leakage inductance was so small that it could be neglected for the analysis of the response of the transformer under load conditions. For this reason, it was omitted in the final diagram of Figure 12. The capacitances were then lumped into a single C, and the resistances combined into a single R. To show the effects upon output voltage wave shape of each of the parameters L, R, and C, the basic transformer is again introduced in Figure 13.

Previously it had been assumed that the magnetizing current was negligible so that a true half-sine of voltage appeared across the transformer terminals. In Figure 13, the magnetizing current is no longer considered negligible in comparison with the current through R. These curves were plotted from equations (1), (1a), (2) and (2a) in Appendix B, Part 1, for a half-sine current source of pulse width 0.1 microseconds. These plots are for typical values of magnetizing inductance when referred to the secondary of a 3:1 pulse transformer with a load resistance of 93 ohms. For a given maximum amplitude of half-sine current excitation, the effect of reducing the magnetizing in-ductance is: (1) to reduce the amplitude of the positive-going output voltage, (2) to shorten the pulse length, and (3) to increase the amplitude of over-shoot. The recovery time of the overshoot is lessened, however, because the initial overshoot amplitude is greater and because the time constant L/R is less. This is an important consideration when the pulse repetition frequency becomes high.

Figure 14 illustrates the effect of capacitance C upon the output wave shape and magnetizing current. Equations (3), (3a), (4) and (4a) of Appendix B, Part 2, were used to plot these curves. The curves for C = 0 are curves 2 of Figure 13, and are used for reference because they have the same values of R and L. The main effect of capacitance C is to delay the rise of the pulse as can be seen from physical reasoning. This has the apparent effect of stretching the pulse width and rounding off the sharp corners of the overshoot peak.

Thus far, the inductance of the transformer has been assumed constant and the analysis confined to a linear network. In Figure 15, the permeability of the material is permitted to change at the peak of the magnetizing current wave shape as was done in Figure 11 for the Basic Transformer. Equations (5) and (6) of Appendix B, Part 3, were used to calculate the response after time $\omega t = \pi$. At this time, the new value of permeability μ' was assumed to change to one-half the value of μ. Actually the magnetizing current peak occurs slightly before $\omega t = \pi$, but for simplicity in calculation this peak assumed at $\omega t = \pi$. (For large C, this error is slight.)

At some later time when the magnetizing current i_m has decreased to less than one-third its peak value, the permeability again changes to a much greater value μ''. In Figure 15, this change is assumed at $\omega t = 2\pi$, and while no calculations were made, the curves are sketched to show a new long-time-constant beyond this point.

The effect of this change in permeability is to cause a "bump" on the overshoot voltage that causes an apparent rapid recovery. However, since the equal area condition must still be fullfilled the curve for constant μ soon crosses the overshoot voltage curve for variable μ.

Figure 15 represents an analytical prediction of the output voltage wave shape of 3:1 pulse transformer with a Ferramic H core designed to replace

the WWI Hypersil-core transformer. The actual response of this transformer
as viewed on an oscilloscope is shown in Figure 23, "93 Ohm Load," and will be
discussed later in Chapter IV. It may be mentioned here, however, that cal-
culated response using the equivalent circuit in Figure 15 gives good correla-
tion with observed response.

Before proceeding to the next section which deals with the actual
3:1 transformer design, the effects of pulse repetition frequency upon voltage
wave shape will be discussed. Consider what happens when a second pulse
follows so close to the first pulse that i_m has not yet decayed to zero. In
terms of the d-c pulse hysteresis loop of Figure 3 (consider R small), this
means that in the B-H plane the next pulse loop will not start at B_r, but rather
at some point still on the return path from B_{max}. The new pulse loop will
then trace out to a region of greater saturation, which means a lower perme-
ability. Not only will the second voltage pulse amplitude be reduced because
of the lower permeability; but since it began before the overshoot of the first
pulse had fully decayed, there will be a downward shift of the base line. A
long sequence of such pulses will cause the material to eventually reach a
quasi-steady state condition somewhere in the first quadrant in the B-H plane
where the resulting magnetizing inductance is low enough and the overshoots
high enough (refer Figure 13) as to cause the areas of the positive portions
of the pulses to be equal to the areas of the negative overshoots. If the
load resistance were very high so that the near-open-circuited hysteresis
pulse loops were executed, the situation could be aggravated since the second
pulse loop would begin almost at B_r' of Figure 3. However, this would require
the pulses to be very close together since the large R condition gives high
overshoots and fast decays. In some very special cases where this situation
arises, the magnetization lag mentioned in Chapter II may have to be con-
sidered.

The extent of voltage amplitude reduction and base line shift is
thus a function of the pulse repetition frequency, the initial overshoot
magnitude, the overshoot decay rate, and the degree of initial saturation in
the material--i.e., how far up the B-H plane the material can go before satura-
tion. If the material is operated over only a small portion of its permis-
sible $\triangle$ B range; and if only a few pulses occur in the pulse chain, then there
may not be a diminution in absolute amplitude of the voltage pulses but merely
a shift in the base line.

D. DESIGN PROCEDURE FOR 3:1 PULSE TRANSFORMERS

It has been shown that there are several factors to be considered
in preparing for a pulse transformer design. These include the nature of the
driving source, the nature of the load, the desired pulse length and con-
figuration, and the pulse repetition frequency. To these factors can be added
the output voltage amplitude desired, the turns ratio, and the core material.
The practical considerations of a suitable winding procedure and the core
mount will also influence the design where large quantities are concerned.

Because the external circuit parameters have such an important
bearing upon the observed output wave shape of a pulse transformer, it is
generally a more practical procedure to be guided by a few fundamental re-
lationships and obtain the optimum performance by experimentation rather than
to attempt a complete design on paper before an experiment is made. The reason
for relying upon experimentation becomes obvious when the designer attempts
to calculate leakage inductance and self capacitance of a pulse transformer.
At best, these calculations can give only orders of magnitude for the small
numbers of turns which are involved here. Thus it becomes necessary to
construct a few sample transformers and measure these unknown quantities.
These measurements together with the observed performance of the pulse trans-
former in a test circuit will then serve to guide the direction for optimum

performance.

If the transformer is to be used in a variety of circuits, the designer must arbitrarily select a typical circuit as his test of performance and base his design upon it. Other circuits may then require minor modifications to adapt to this design.

In the case of the 3:1 design for WWI application, the problem was to develop a ferrite-core pulse transformer which could replace an existing Hypersil-core model. The problem was well defined in that the circuit applications were known and the existing Hypersil transformer could be used as a standard for performance measurement. To illustrate a procedure which may be followed under such circumstances, the actual design of an acceptable ferrite-core 3:1 pulse transformer is carried out.

To simulate the conditions of operation, a Basic Point-To-Point Amplifier Circuit as shown in Figure 20 was selected. From this circuit, and from the general operating requirements in WWI, the following specifications for the design were established:

1. The pulse shape is 0.1 microsecond, half-sine.

2. The maximum pulse repetition frequency is 2 megacycles.

3. The output pulse amplitude is to have a maximum value of 20 volts peak, the transformer being 3:1 stepdown.

4. The driving source is a power pentode which may be considered as a current source.

5. The load resistance can be considered as 93 ohms, referred to the secondary.

6. The total circuit capacitances, exclusive of the transformer, are 10 mmf in the primary, and 50 mmf in the secondary.

From these specifications, the pulse transformer was to fulfill these requirements:

1. Pass the half-sine pulse with as little distortion as possible.

2. To have as small a pulse-repetition-frequency sensitivity as possible—i.e., to have as little diminution in amplitude and shifting of base line for a train of pulses as possible.

3. To be of small size and easily mountable.

4. To be capable of manufacture at a reasonable cost.

For a core shape, a small toroid of dimensions approximately 3/8" outside diameter, 3/16" inside diameter and 1/8" thick was selected. The material used was Ferramic H. It was decided to base the design upon the pulse-repetition-frequency sensitivity requirement. This is related to the magnetizing inductance L of the transformer in the following development, using the equivalent circuit of Figure B-1, Appendix B.

Let T = half-sine pulse width   = 0.1 microsecond

   T' = time between pulses in seconds = 0.4 microseconds

   τ = time constant of recovery voltage = L/R.

In a time period of 4 time constants, a simple exponential will have decayed to less than 2% of zero.

Let τ = $T'/4$ = 0.1 microseconds

Since R = 93 ohms,

   L = τR = 9.3 microhenries, referred to the secondary.

From equation (7), Appendix B, Part 4,

$$N_s = \sqrt{\frac{L\, l_m\, 10^8}{0.4\pi\, A\mu_e}} = \text{number of secondary turns.}$$

From the core measurements and the value of μ_e = 450 (Table 1):

   l_m = 2.24 cm

   A = 0.076 cm^2

So that

$$N_s = \sqrt{\frac{9.3 \times 2.24 \times 10^2}{0.4\pi \; 0.076 \times 450}} = 6.96$$

Using $N_s = 7$, $N_p = 3 \times 7 = 21$ primary turns.

Recalculating the inductance L,

L = 9.4 microhenries, referred to the secondary.

Since $\psi = \tan^{-1} \frac{R}{\omega L} = \tan^{-1} \frac{93}{2\pi 10^{+7}(9.4)10^{-6}} = 17\text{-}1/2^{\circ}$,

curve 2 of Figure 13 applies, with capacitance and non-linearity not yet considered.

An approximation of the maximum flux density, B_{max}, for the operating conditions can be made using Formula (8) of Appendix B, Part 4,

$$\Delta B_{max} = \frac{2 \; E_t \; T \; 10^8}{\pi \; NA}$$

For $E_t = 20$ volts,

$$\Delta B_{max} = \frac{2 \; (20) \; (0.1)10^2}{\pi \; (7) \; (0.078)} = 233 \text{ gauss.}$$

This figure will be high, because the **actual voltage** shape across the transformer requires less flux than a 0.1 microsecond half-sine.

From Table 1 or Figure 8, it is seen that the material will be well below saturation.

There is no accurate method of calculating the distributed capacitances and leakage inductance of this shape of toroid with so few turns, so these values were measured after the core was wound with 21 and 7 turns of No. 36 Double Formex Wire. To keep the leakage inductance small, the primary and secondary were concentrically wound.

Measurements on a Q-meter gave the following readings at 5 mcs.

C_m = winding-to-winding capacitance = 8 mmf.

C_p = primary distributed capacitance = 2 mmf.

$\mathcal{L}$ = leakage inductance (short circuit inductance), too small to be measured.

Referring all the capacitances to the secondary:

$$C = 9(C_p + C_{source}) + C_m + C_{load} = 9(2 + 10) + 8 + 50 = 166 \text{ mmf.}$$

A check is made to insure that the roots of the characteristic equation of the R,C,L parallel combination are real (see Appendix B, Part 2).

$$\left(\frac{1}{2RC}\right)^2 = \frac{1}{(2 \times 93 \times 166 \times 10^{-12})^2} = 10.5 \times 10^{14}$$

$$\frac{1}{LC} = \frac{1}{9.4 \times 166 \times 10^{-18}} = 6.4 \times 10^{14}$$

Since $\left(\frac{1}{2RC}\right)^2 > \frac{1}{LC}$, the overshoot will be overdamped, which is the situation desired.

An analytical plot of the output wave shape for the transformer parameters will give a curve similar to those of Figure 14. Because a curve for C = 166 mmf is not shown, the curve for C = 90 mmf will be used to illustrate the calculation of B_{max}. (for the calculations below, this value is not much in error.)

From Figure 14 for C = 90 mmf, the maximum positive voltage e_{tm} = 72 I. Also, I_m = maximum i_m = .42 I. Hence, I_m = .0058 e_{tm}, referred to the secondary.

For $e_{tm} = 20^v$, $I_m = (.0058 \times 20) = .116$ amps.

$$\Delta B_{max} = \mu_e \; \Delta H = \frac{0.4\pi N I_m}{l_m} \mu_e = \frac{0.4\pi(.116)(450)}{2.24} = 205 \text{ gauss.}$$

To produce 20 volts across the 93 ohm load resistor, the current source must be capable of providing a peak current of:

$$I = 20/72 = .278 \text{ amperes, referred to the secondary,}$$

or

$$I_p = .278 \times 1/3 = 92 \text{ ma in the primary.}$$

The effect of non-linearity in L will produce a change in the shape of the overshoot similar to that shown in Figure 15. For this low value of ΔB_{max} however, the change in permeability will not be as great as the 2:1 change pictured in Figure 15.

For computing values of B_{max} and current source requirements, little error is introduced by using the curves of Figure 13, provided the capacitive loading is not excessive.

The actual construction and circuit operation of this transformer design will be discussed in Chapter IV. It should be noted from curve 2 of Figure 13, however, that the magnetizing current near the end of the pulse rises to a value which is over 40% of the peak supply current. For square pulses, the usual criterion is a maximum magnetizing current of 10% of the peak supply current. Applying this condition to the half-sine pulse would result in curve 5 of Figure 13 which has a small amplitude overshoot with a long-time decay.

The next section will deal with the design of a 1:1 pulse trans- former for WWI circuitry. In this case, the transformer is operated under open-circuit conditions and is allowed to "ring." Because the leakage inductance plays such an important part in determining the ringing character- istic, a different equivalent circuit is used for the 1:1 design than the simple L,R,C parallel combination used in the 3:1 design.

E. THE 1:1 PULSE TRANSFORMER EQUIVALENT CIRCUIT

The most common application for 1:1 pulse transformers in WWI is for local point-to-point coupling between two amplifiers adjacently located. Here the secondary of the transformer is coupled directly to the grid of the adjacent amplifier with no load termination. This gives a high amplitude to the positive pulse as the transformer parameters combine with the external circuit constants to produce a resonant "ringing" effect. (See Figure 26)

Because only the first positive pulse is desired, a diode is connected
across the transformer so that on the negative swing a low resistance load
is present. This causes the circuit to suddenly become overdamped on the
negative voltage swing and the energy of the circuit is dissipated in the diode
forward resistance. (Actually a small resistance is included in series with
the diode in order to produce the desired amount of damping.)

In applying the 1:1 Hypersil-core pulse transformer in the manner
described above, it was found that in spite of the damping diode an external
shunt inductance of about 50 microhenries was necessary across the transformer
terminals in order to prevent the recurrence of positive pulses. An analysis
of the circuit with the external shunt inductance was difficult due to the
non-linear behavior of the Hypersil core at these high frequencies. In
ferrites, however, the eddy currents are very small and it was found that an
equivalent circuit could be developed which would not only show the oscilla-
tion frequencies involved but would also explain the action of the external
shunt inductance. This equivalent circuit will now be discussed.

Because the leakage inductance plays such an important part in
determining the ringing frequencies of the 1:1 pulse transformer, it is
necessary to include it in the circuit development. Consider the 1:1 trans-
former as a coupled circuit as shown at the top of Figure 16. Here L_1
represents the primary self-inductance and M the mutual inductance between the
two circuits. Because this is a 1:1 transformer, the secondary self-inductance
is numerically equal to L_1. C_1 and C_2 represent the sum of all the capacitances
on the primary and secondary respectively.

Defining a "leakage coefficient" $\sigma = (1 - \frac{M^2}{L^2})$, the transformer
equivalent circuit can be drawn as shown in the second diagram of Figure 16.[5]

5. Guillemin, E. A., <u>Communication Networks</u>, Vol. 1, pp. 310-323, John Wiley &
Sons, 1931.

If the resistances are then omitted, the third diagram results where ℓ = sum of the primary and secondary leakage inductances = $L_1 \sigma$, and L = magnetizing inductance = $L_1 (1-\sigma)$.

For clarity the current source I is now replaced with a voltage source $V = \frac{1}{C_1} \int I \, dt$, and the equivalent circuit for the 1:1 pulse transformer with no load is complete.

Inspection of this new circuit shows that it consists of a voltage source supplying a series resonant circuit ℓC_1 and a parallel "anti-resonant" circuit LC_2. The resonant and anti-resonant frequencies are defined as f_1 (or ω_1) and f_2 (or ω_2) respectively.

Figure 17 illustrates the use of susceptance plots for determining the natural behavior of the transformer equivalent circuit. The ratio of output voltage E_2 to driving source voltage V or "transmission" $T(j\omega)$ is equal to the admittance of the series circuit Y_1 divided by the sum of the admittances of the series and parallel circuits $Y_1 + Y_2$. The poles (infinities) of $T(j\omega)$, which are the oscillation frequencies of the network, are determined by finding the zeros of the sum of the admittances $Y_1 + Y_2$. This may be done graphically by adding the two separate admittance plots for Y_1 and Y_2 as shown in Figure 17. The natural frequencies or oscillation frequencies of the network are then defined as ω_R' and ω_R''. Note that ω_1 and ω_2 lie between the natural frequencies of the network.

In Appendix C, Part 1, these oscillation frequencies are shown to be equal to:

$$\omega_R'' = \sqrt{\alpha + \sqrt{\alpha^2 - \beta}} \tag{12}$$

$$\omega_R' = \sqrt{\alpha - \sqrt{\alpha^2 - \beta}} \tag{13}$$

where, $2\alpha = \frac{1}{\sigma L C_2} + \frac{1}{\ell C_1}$ (10)

and $\beta = \frac{1}{\ell L C_1 C_2}$ (11)

If the transformer is now driven from a current source having a half-sine pulse shape, the output voltage E_2 may be calculated. The transient response to this excitation is calculated in Appendix C, Part 2, and the results are given by equations (14) and 18) for the periods during the driving source pulse length and after the driving source pulse termination respectively.

For $0 \le \omega t \le \pi$,

$$E_2 = IK\left[\frac{\cos y\omega t}{(x^2-y^2)(1-y^2)} + \frac{\cos x\omega t}{(x^2-y^2)(x^2-1)} - \frac{\cos \omega t}{(x^2-1)(1-y^2)}\right] \quad (14)$$

For $\pi \le \omega t$,

$$E_2 = KI\left[\frac{\cos y\omega t + \cos y(\omega t-\pi)}{(x^2-y^2)(1-y^2)} + \frac{\cos x\omega t + \cos x(\omega t-\pi)}{(x^2-y^2)(x^2-1)}\right]$$

Where $\quad K = \dfrac{1}{\rho C_1 C_2 \omega^3}$ \hfill (15)

$$x = \frac{\omega_R''}{\omega} \quad\quad\quad (16)$$

$$y = \frac{\omega_R'}{\omega} \quad\quad\quad (17)$$

In these expressions I is the maximum amplitude of the current pulse and ω is the fundamental frequency component of the driving source, i.e., for 0.1 microsecond half-sine pulse $\omega = 5$ megacycles.

Plots of the transient response of the 1:1 pulse transformer equivalent circuit for various values of x and y are given in Figure 18A. These curves may be used to point the direction for proper values of x and y to give a desired response. An important point to be observed is the pulse delay introduced when the pulse transformer is operated under these open-circuit conditions (compare the curves of Figure 18A with those of Figure 13).

The type of analysis which has been presented here will be used in the next section to predict the behavior of a ferrite-core 1:1 pulse transformer which was designed to replace the standard WWI Hypersil-core transformer.

The effect of adding an external shunt inductance or "tail-reversing inductance" will be included in the analysis.

F. DESIGN PROCEDURE FOR 1:1 PULSE TRANSFORMERS

As in the case of the 3:1 design, the 1:1 ferrite-core pulse transformer was designed to replace an existing model—in this case the WWI standard 1:1 transformer with a Hypersil core. In the original design the Hypersil pulse transformer was specified to work into a load of 1,000 ohms.[1] However, it was found that a higher amplitude pulse could be obtained by operating the transformer open-circuited. Because the resultant ringing occurred partially above the base line so that a damping diode was not effective in preventing the recurrence of a positive pulse, (see Figure 26 "S_1 Open S Closed"), an external shunt inductance called "Tail Reversing Inductance" was added. The effect of this inductance is to reduce the L of Figure 17 so that ω_2 and hence ω_R' are increased. Thus after the first pulse the ringing occurs below the voltage reference line where the damping diode is effective in "clipping" the pulse.

Following the procedure for the 3:1, a test circuit was built which would simulate a typical operating condition. This circuit is shown at the top of Figure 20 and will be discussed in more detail in the next chapter. Because the relative importance of the pulse transformer parameters had never been developed for this application, it was necessary to use an experimental approach to match the performance of the ferrite-core transformer with that of the Hypersil transformer. In doing this, it soon became apparent that the existance of a finite amount of leakage inductance was essential to the transformer's operation. Because a toroidal shape had been selected for purposes of standardization with the 3:1 design, it was necessary to separate the windings to introduce this leakage. Based on the observed performance

---

1. Ibid.

of the Hypersil 1:1 transformer, the requirements set forth for the 1:1 ferrite design were then as follows:

1. The driving force is a half-sine current pulse of 0.1 microsecond duration.

2. The maximum pulse repetition frequency is 2 megacycles.

3. For the test circuit of Figure 20, the output pulse amplitude is to be 20 volts peak.

4. The combination of a damping diode-and-resistor together with a 50 microhenry tail reversing inductance must prevent the recurrence of another positive swing after the initial positive pulse.

5. For purposes of standardization, the geometrical shape of the 1:1 transformer and the 3:1 transformers are to be the same.

In the case of the 1:1 transformers, the pulse-repetition frequency sensitivity was not to be the basis of design since the overshoot is a double frequency transient which cannot be resolved into a simple exponential decay. Instead, the two-humped overshoot of the Hypersil transformer was duplicated by experimentation with a ferrite-core transformer, (see Figure 26, "S_1 and S Closed").

This ferrite-core transformer is a Ferramic H toroid of the same dimensions as the 3:1, and has two windings of 24 turns of No. 36 Double Formex wire wound on opposite quadrants of the toroidal shape. From measurements on a Q-meter, the transformer capacitances and leakage inductance were found to be:

$$C_p = C_s = 5 \text{ mmf.}$$

$$L_1 \sigma = 15 \text{ microhenries.}$$

From formula (7) of Appendix B, Part 4, for 24 turns, and $\mu_e = 450$

$$L_1 = \frac{0.4\pi N^2 A \mu_e 10^{-8}}{l_m} = \frac{0.4 \pi (24)^2 (0.078) (450) 10^{-8}}{(2.24)} = 110 \text{ microhenries}$$

Thus $\sigma = \dfrac{15}{110} = 0.13.$

From measurements taken on the test circuit (including oscilloscope probe), primary capacitance exclusive of the transformer = 18 mmf, and secondary capacitance (without tail-reversing inductance) = 52 mmf.

Using the equivalent circuit developed in Figure 16 and the mathematical expressions for output voltage derived in the last section, the response of this transformer was calculated for the conditions without the external shunt inductance and with the external inductance. Without the inductance, the following parameter values apply to Figure 16:

$$L = L_1(1-\sigma) = 110 - 15 = 95 \text{ microhenries.}$$

$$\ell = 15 \text{ microhenries}$$

$$C_1 = 5 + 18 = 23 \text{ mmf.}$$

$$C_2 = 5 + 52 = 57 \text{ mmf.}$$

From the relationships derived in Appendix C, Part 1,

$$\omega_1 = \frac{1}{\sqrt{\ell C_1}} = 5.4 \times 10^7$$

$$\omega_2 = \frac{1}{\sqrt{L C_2}} = 1.36 \times 10^7$$

$$\alpha = \frac{\omega_2^2 + \omega_1^2}{2} = 2.16 \times 10^{15}$$

$$\beta = \omega_1^2 \, \omega_2^2 = 53.6 \times 10^{28}$$

$$\omega_R'' = \sqrt{\alpha + \sqrt{\alpha^2 - \beta}} = 6.45 \times 10^7$$

$$\omega_R' = \sqrt{\alpha - \sqrt{\alpha^2 - \beta}} = 1.14 \times 10^7$$

$$X = \frac{\omega_R''}{\omega} = 2.05$$

$$y = \frac{\omega_R'}{\omega} = 0.36, \text{ where } \omega = 2\pi(5 \times 10^6).$$

Expressions (14) and (18) of Appendix C, Part 2, were then calculated. In these expressions, $K = \frac{1}{\ell C_1 C_2 \omega^3} = 1.64 \times 10^3$. These expressions are plotted in Figure 18B by the solid curve. In this plot the value of K is reduced to 10^3

so that the voltage value at any point is given in terms of the peak value of supply current as expressed in ma.

For $E_{2\ max}$ = 20 volts, I = 20/0.9 = 22 ma. Considering all the current as magnetizing current, an approximation for the ΔB_{max} is given by,

$$\Delta B_{max} = \mu_e\ \Delta H = \frac{0.4\pi NI\mu_e}{l_m} = \frac{0.4\pi(24)\ (22)\ (450)\ 10^{-3}}{2.24} = 133 \text{ gauss},$$

so that the core is well below saturation.

Next the 50 microhenry tail-reversing inductance L_t was considered to be in parallel with L, as shown in the top of Figure 18B with switch S closed. Measurements showed that this inductance had a distributed capacitance of 4 mmf, so this was combined with C_2 to give the following new values for the 1:1 equivalent circuit:

C_1 = 23 mmf.

C_2 = 57 + 4 = 61 mmf

$\mathcal{l}$ = 15 microhenries

$L = \dfrac{50 \times 95}{50 + 95} = 32.8$ microhenries

$\sigma = \dfrac{15}{15 + 32.8} = 0.314$

From these new parameters the natural frequencies of resonance are found:

$\omega_1 = 5.4 \times 10^7$

$\omega_2 = 2.24 \times 10^7$

$\alpha = 2.25 \times 10^{15}$

$\beta = 1.45 \times 10^{30}$

$\omega_R{}'' = 6.45 \times 10^7$

$\omega_R{}' = 1.85 \times 10^7$

$x = 2.05$

$y = 0.59$

$K = 1.54 \times 10^3$

Note that the addition of the shunt inductance L_t has little effect upon the high frequency ω_R'', but increases ω_R'. The dashed curve of Figure 18B shows the calculated response. Here again the plot is given on the same scale as the solid curve so that K for the diagram is 10^3.

Figure 18B may be compared with the observed performance in Figure 26 for Ferramic H, and it will be seen that there is good correlation between the calculated response and the observed response. The effect of the shunt inductance L_t in increasing ω_R' has caused the "ringing" frequency ω_R'' to be contained below the voltage base line after the initial positive pulse. The effect of the damping diode is then to overdamp ω_R' sufficiently to prevent the recurrence of a positive pulse.

CHAPTER IV

PULSE TRANSFORMER CONSTRUCTION AND TEST

A. CONSTRUCTION OF PULSE TRANSFORMERS

There are three general geometric shapes which are available for pulse transformer construction. These are the C-shape, the cup core, and the ring or toroidal shape. The C-shape is advantageous when an air gap is desired and has the further advantage of permitting the use of coil forms for the windings. The disadvantage of the C-shape is that it requires a clip of some kind to hold the C-shapes together.

The cup core is being used extensively for small pulse transformers by several manufacturers because of the relative ease in assembly as compared with the C-shape. The typical procedure is to provide a hole through the center of the cup shapes so that a mounting screw may be inserted for clamping the two halves of the cup shape together. The disadvantage of the cup core is its relative high cost. For WWI the cup core had the further disadvantage that the leakage inductance could not be controlled as easily as the C-shape or toroid. A further disadvantage is the necessity of bringing the coil leads out of the cup without lead-to-core breakdown.

For WWI the toroid had the advantage of small size, low cost, and ease of control of leakage inductance. The difficulty in winding procedure was in a large measure reduced by the concurrent development in the Laboratory of a toroidal winder which could handle the small 3/16" inside diameter ring.* For these reasons the toroidal shape was selected for the 3:1 and the 1:1 ferrite-core pulse transformers.

---

* This winder and the assembly technique for the pulse transformers were developed by Mr. Robert Hunt of the Digital Computer Laboratory, M.I.T.

Figure 19 shows the assembly of a 3:1 pulse transformer. The toroidal shaped core was first put through a tumbling mill to knock down the sharp corners and then the core was coated with enamel to prevent chafing of the wire during winding. The primary and secondary windings were then placed on the core. For the 3:1 transformers the windings were concentrically wound, which for the 1:1 transformers the coils were placed on opposite quadrants of the ring. The wound transformer was then placed in a phenolic mounting board which contained the heavy pigtails for external connection. After soldering the transformer wires to the pigtails the whole assembly was placed in a die and a thermo-setting plastic resin used to mold a protective cover over the transformer. The complete transformer which measures 3/4" x 3/4" x 3/8" resembles a condenser with four pigtails.

B. TEST CIRCUITS FOR PULSE TRANSFORMERS

In the preceding chapter on design mention was made of the test circuits which were used as the basis for determining the performance of the 3:1 and the 1:1 pulse transformers. These circuits were selected as being a typical application for the transformers in WWI and were constructed into a test panel for rapid transformer testing. The circuits are shown in Fig. 20 and will be discussed now in order of their appearance from top to bottom.

The 1:1 pulse transformer circuit is a basic gate tube circuit. In normal operation a gating pulse will be applied to the suppressor which permits the input pulse to appear across the tube output. For the test circuit this suppressor was grounded to the cathode. Two switches were provided to permit the observation of output waveshape with and without the damping diode and with and without the tail reversing inductance.

The 3:1 pulse transformer circuit is a basic point-to-point amplifier circuit using a power pentode with a 250-volt plate supply. In this

circuit a damping diode was connected through a switch across the primary
of the transformer to demonstrate the increased sensitivity to pulse repe-
tition frequency when the overshoot is clipped. Not shown in the diagram
is a 93-ohm resistance load across the transformer output.

Also included on the test panel was a gate generator output amplifier
circuit which is used for checking 5:1 pulse transformers. (This thesis does
not include a design for 5:1 transformers. In application these transformers
are driven by square pulses in the order of 0.5 microsecond duration.)

Figure 21 is a block diagram of the equipment used for supplying
the input pulses to the test circuits. A variable-frequency clock-pulse
generator provides a constant series of half-sine pulses of 0.1 microsecond
duration. For most of the test work the pulse repetition frequency was set
at 2 megacycles. The output of the clock-pulse generator was fed to a scope
synchronizer where a frequency division occurs to produce positive pulses
for triggering the synchroscope. The internal trigger delay of the synchro-
scope was used to provide an adjustable delayed pulse to a gating pulse
multivibrator of a pulse gater. The gate tube of the pulse gater received
the gate pulse on its suppressor and a clock-pulse on its control grid. The
resultant chain of 0.1-microsecond half-sine pulses were then fed through the
pulse amplifier of the pulse gater and then to the pulse transformer test
panel.

Figure 22 shows the complete test set-up, excluding the synchroscope.
The transformer connections were brought out to four-terminal Jones plugs
which were mounted in the front of the panel. Thus the experimental cores
could be quickly tested using a standard plug-in jig.

C. TEST RESULTS

Figure 23 shows a comparison of various ferrite materials used for
the core of a 3:1 pulse transformer. These materials were wound with 21 and

7 turns and the output waveshapes are shown under various load conditions with the WWI Hypersil-core transformer as a reference. Considering the open circuit condition first, the leakage inductance in the WWI transformer is seen to produce a small ripple or oscillation on the waveform which is absent in the other transformers. Also, the eddy-current losses in the WWI Hypersil transformer produce a greater damping effect on the low frequency oscillation than that which occurs in the ferrite transformers. The effect of a decreased pulse permeability is shown in the comparison of the Ferramic H, Ferricore, and MF1131. These materials have pulse permeabilities of 450, 230, and 40 respectively, and the resultant decrease in positive pulse amplitude and increase in overshoot amplitude are noticeable. MF1131 is the square loop material with the long time lag mentioned in Chapter 2, and it is significant that the low frequency oscillation is more effectively damped than Ferricore.

When a 93-ohm resistive load is connected across the terminals of the transformer the normal operating conditions are simulated. The Ferramic H transformer produces the type of overshoot which was desired in order to give recovery before the next pulse. The Ferricore and MF1131 transformers have faster recovery times but at the expense of positive pulse amplitude reduction.

If a damping diode is connected across the transformer, the overshoot is "clipped". While this appears to be an advantage it is only necessary to recall that the recovery time constant is L/R, where R is the total resistance across the transformer during overshoot, to realize that such a diode will produce increased sensitivity to pulse repetition frequency. This is brought out in Fig. 25 where the effect of the damping diode on a chain of pulses is observed. With the diode in the circuit there is a decay in positive pulse amplitude which is absent when the diode is absent. This

effect is even more noticeable in Fig. 24 where the integrated output is shown for the cases with and without the damping diode. With S closed, the diode is in the circuit and the integral of v_t is seen to approach zero much slower than with S open.

Figure 26 shows the output waveshapes of the 1:1 pulse transformer made of Ferramic H as compared to the WWI standard which has a Hypersil core. The Ferramic H waveshapes are in close agreement with the analysis of Chapter III, and the waveform is seen to be a good approximation to the WWI standard tail reversing inductance and the damping diode are in the circuit. In the case of the 1:1 transformers, the recovery time with the diode in is sufficiently fast so that the pulse repetition frequency sensitivity is not of concern.

From Figs. 23 to 26 it can be seen that pulse transformers made with ferrite cores can be designed to replace the Hypersil ones. Although the cores used in the design were Ferramic H, other materials such as Ferroxcube 3C, Ceramag 5N and Ceramag 7A will perform equally as well. The final selection of material from this representative group may then be based primarily on cost.

In the 1:1 transformers, it is possible to "build" the tail reversing inductance into the transformer by using a lower permeability core material than Ferramic H. Experiments made with Ferricore indicate that this material has about the right value of pulse permeability to provide the decrease in self-inductance that is required. (Because the leakage inductance depends upon geometry, using the same toroidal shape and winding scheme thus permits the leakage inductance to remain constant.)

CHAPTER V

SUMMARY

The main objective set forth for this thesis research was to determine if the new ferrites could be used as core materials for pulse transformers for WWI. The research consisted of (a) determining the magnetic behavior of the ferrites under pulse conditions, (b) developing an equivalent circuit which could be used to predict the response of the pulse transformer under WWI conditions, and (c) designing and testing ferrite-core pulse transformers. The method of attack and the results obtained from each of these three parts of the research will now be summarized.

A. DETERMINING THE MAGNETIC BEHAVIOR OF FERRITES UNDER PULSE CONDITIONS

Apparatus was constructed to perform pulse tests on the ferrite materials. This equipment consisted of a gas-tube pulse generator which provided a variable pulse width of from 0.1 to 0.3 microseconds of half-sine current for the core excitation. Using a standard procedure of integration and amplification through video amplifiers, the pulse loops were presented upon a cathode-ray tube and quantitative measurements of ΔB vs. ΔH taken. When these data were compared with data taken from slow-speed pulse excitations, it was found that there was good correlation. This indicates that at the 0.1 microsecond pulse widths the eddy current effects are small and the ferrite material can be judged on the basis of its d-c characteristics. Values of pulse permeabilities were then given which can be used in pulse transformer design. It was shown that for pulse widths less than about 0.5 microseconds the ferrite materials have higher pulse permeabilities than grain-oriented steels.

The disadvantages of the ferrites for pulse transformer applications was pointed out to be (a) low saturation values, and (b) low Curie temperatures.

For the application in WWI, however, these disadvantages are not particularly important.

B. DEVELOPMENT OF PULSE TRANSFORMER EQUIVALENT CIRCUITS

Because the two transformer designs presented in this thesis involved entirely different operating conditions, two separate equivalent circuits were developed. For the 3:1 pulse transformer which operates into a low-resistance load, the leakage inductance was made small in order to prevent attenuation of the output voltage. This permitted the circuit representation by a simple LRC parallel combination for the 3:1 transformers.

For the 1:1 pulse transformer which operates essentially open-circuited, use is made of the natural frequencies of oscillation of the transformer to produce a large positive pulse. For this reason, the leakage inductance is purposely made finite and the equivalent circuit for the 1:1 pulse transformers, which consists of a series ℓ C_1 in combination with a parallel LC_2, includes this element.

Before the actual equivalent circuits were developed a "Basic Transformer" was introduced. This consisted of a pure lossless inductance and it was used to illustrate the relation between the voltage-time plane and the B-H plane. Effects of non-linearity in inductance were shown for the conditions of no-load and full-load on the Basic Transformer.

Following the introduction of the equivalent circuit for the 3:1 pulse transformer, analytically derived curves were presented which could be used in the design procedure. These curves show the effects of resistive loading upon output voltage wave shape and magnetizing current for the conditions of a half-sine excitation. The effect of capacitance upon output wave shape was included and a hypothetical case of non-linearity in inductance was similarly shown.

In WWI, advantage is taken of resonant frequency peaking in the 1:1

pulse transformers when operated under no-load conditions. For this reason, the 1:1 pulse transformer equivalent circuit was developed with the objective being to disclose the nature of the natural frequencies of oscillation in these transformers. Two methods were then presented for determining these oscillation frequencies. One consisted of a graphical method of susceptance plots while the other was an analytical method. Formulae were then developed for determining the output wave shape of the 1:1 pulse transformer under no-load conditions when driven from a half-sine current source. From these formulae, curves were plotted of the output voltage wave shape for various ratios of the resonant frequencies of the transformer to the fundamental frequency of the driving source. These plots serve as a guide to indicate the proper direction in a design.

C. DESIGN AND TESTING OF FERRITE-CORE PULSE TRANSFORMERS FOR WWI

Using the equivalent circuits, a design procedure for a 3:1 pulse transformer to replace the Hypersil-core transformer in WWI was presented. This design was based on a low pulse repetition frequency sensitivity criterion. The response of this design was then compared to the Hypersil core and shown to be compatible. Effects on pulse repetition frequency sensitivity of a damping diode were also shown.

In the 1:1 pulse transformer design, the criterion was to duplicate the voltage wave shape of the WWI Hypersil model when a damping diode and tail reversing inductance were placed across the transformer. In order to do this, it was necessary to determine experimentally the required number of turns. From the computed values of self-inductance and measured values of leakage inductance and circuit capacitance, the wave shape of the ferrite-core transformer was then determined analytically and shown to closely resemble the observed actual response. The equivalent circuit was thus shown to be adequate for this application and will be valuable in predicting the performance of

the 1:1 transformer under circuit conditions other than that for which the transformer was tested. The 1:1 equivalént circuit is further helpful in bringing out the fact that to eliminate the tail reversing inductance one needs to keep the leakage inductance the same while reducing the self-inductance of the transformer. Since both inductances are proportional to the square of the turns, the way to do this is to use a ferrite with a low value of pulse permeability.

The method of fabricating the ferrite-core transformer was shown where a thermo-setting plastic resin is used to cast a protective coating around the unit. The resultant transformer then becomes small in size, light in weight and easily mountable. No figure was given for the comparitive costs of the ferrite-core transformers and the Hypersil-core transformers because complete figures were not yet available at the writing of this thesis. It is expected, however, that the ferrite-core transformer will cost only a fraction of that of the metallic-core pulse transformer.

In conclusion, it can be stated that the ferrite-core pulse transformer appears to be admirably suited for 0.1 microsecond pulse applications in WWI. There are at least four and possibly more ferrite materials which are suitable for this work and the question of selection becomes simply a question of price. With regard to the shape of core, the designs presented here were based on a ring or toroidal shape. However, having determined the nature of the problem and found the resultant equivalent circuit and parameter values necessary to produce the desired results, there is no reason to believe that other shapes such as C-type and cup-core type could not be used. In this research, some difficulty was found in controlling the leakage inductance from the negigible value required in the 3:1 design to the comparitively large value needed in the 1:1 design when a cup core was used. (For purposes of standardization, the shapes for the 1:1 and the 3:1 pulse transformers should

be the same.) In the C-shape, however, the primary and secondary windings

may be placed on opposite legs to introduce the necessary leakage inductance

for the 1:1 design. Specifications for a C-shape core were drawn up at the

beginning of this thesis work, but unfortunately samples had not yet arrived

at the writing of this report.

Signed..Richard.D..Robinson.

Approved................................

Jay W. Forrester

APPENDIX A

APPARATUS FOR TAKING PULSE HYSTERESIS LOOPS

In order to generate half-sine pulses of variable amplitude and pulse width for supplying the H excitations to ferrite cores, the circuit of Figure 1 was constructed. In the plate circuit of the 2D21 hydrogen thyratron, the switch S selects an inductance which together with capacitor C determines the time duration of the generated pulse. A 100,000 ohm potentiometer in the plate supply determines the pulse amplitude, while the 200,000 ohm series resistor is necessary for isolating the plate circuit from the supply during the period of tube conduction.

To drive the generator, a pulse from a P-5 Synchroscope was used at a repetition frequency of 4,000 cycles per second. This pulse was differentiated in the grid circuit to give a sharper peak, the differentiating circuit consisting of the 68 mmf condenser and 10,000 ohm resistor. An additional 10,000 ohm resistor was placed in series with the grid to prevent excessive grid current flow.

The sample was placed in the cathode circuit of the pulse generator along with resistor R_1 for measuring H and the integrating circuit R_2 and C_2 for providing a voltage proportional to B. The value of R_1 was experimentally adjusted to cause its voltage drop to be approximately 3% or less of the total voltage across the sample. For this reason, the integrator can be considered to be effectively across the sample alone. The value of the integrator elements was determined by placing a minimum load condition of 10,000 ohms across the sample winding and to give an integrating time constant of 3.3 microseconds. For 0.1 microsecond pulses which have a fundamental frequency component of 5 megacycles, the integrating $\omega RC = 16.5$ is well above the $\omega RC \simeq 10$ which is necessary for better than 1/2% accuracy. Although it would have been desirable

to increase R_2 to 100,000 ohms, this would have necessitated C_2 being 33 mmf,
a value comparible with stray capacitances.

The voltages from C_2, representing B, and from R_1, representing
H, were then amplified through two video amplifiers with identical time delays.
For this purpose, two Tektronix 514D scopes were matched, the amplifier of
one being used to drive the horizontal plates of the other. Since for the
size of the sample and the number of turns used, the values of B and H
voltages were in the same range of magnitude, this proved to be a workable
method. The scopes were oriented with respect to each other in such a manner
as to permit the use of short intra-connection leads. Although the manufacturer
specifies a bandwidth of 10 mc. for these scope amplifiers, this is not an
unreasonable value since the H-wave shape is half-sine with a fundamental
frequency of 5 mc. The B-voltage bandwidth requirements are of course not
as stringent since this is an integral. For reasons of amplifier distortion
it is to be expected that the pulse hysteresis loops will not show their
true sharp corners.

The calibration of this equipment was extremely simple since the
oscilloscopes were provided with voltage calibration controls. The following
formulas were used to calculate B and H:*

$$H = \frac{4 \, N \, v_1}{10 \, l_m R_1} \quad \text{oersteds}$$

$$B = \frac{10^8 \, R_2 C_2 v_2}{NA} \quad \text{gauss}$$

l_m = mean magnetic path (cm)
N = number of turns
v_1 = voltage across R_1 (volts)

v_2 = voltage across C_2 (volts)
A = cross-section area of sample (cm^2)
$R_2 C_2$ = integration time constant (sec)

---

*Glasoe and Lebacqz, Pulse Generators, Rad. Lab. Series No. 5, p. 642, McGraw-
Hill Book Company, 1948.

APPENDIX B

3:1 PULSE TRANSFORMER EQUATIONS

1. DERIVATION OF EQUATIONS FOR PLOTTING FIGURE 13
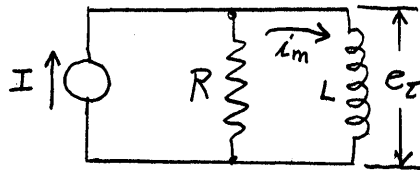
Fig. B-1
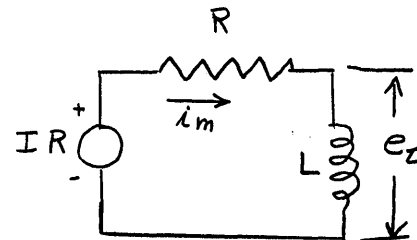
Fig. B-2

Figure B-2 is equivalent to Figure B-1. In both figures, all values are referred to the secondary of the transformer. Writing the loop equations for Fig. B-2 in Laplace Transforms:

$$\frac{LsI(s)}{(Ls+R)} = E_t(s)$$

Since $I(s) = \frac{IR\,\omega}{s^2+\omega^2}(1+e^{-\frac{\pi}{\omega}s})$, (the transform of a half-sine pulse),

$$E_t(s) = \frac{sIR\,\omega}{(s+R/L)(s^2+\omega^2)}(1+e^{-\frac{\pi}{\omega}s}) \triangleq E_1(s)+E_2(s)$$

and

$$I_m(s) = \frac{E_t(s)}{Ls}$$

From Formula 1.210, Gardner and Barnes[*];

For $0 \leq \omega t \leq \pi$

$$e(t) = E_1(t) = \frac{-IR^2\omega L}{R^2+(\omega L)^2}e^{-\frac{R(\omega t)}{\omega L}} + \frac{\omega L IR}{\sqrt{R^2+(\omega L)^2}}\sin(\omega t+\psi) \quad (1)$$

$$\text{where } \psi = \tan^{-1}\frac{R}{\omega L} = \tan^{-1}\frac{R}{X}$$

---

[*] Gardner and Barnes: <u>Transients in Linear Systems,</u> John Wiley & Sons, 1942

and

$$i_m = \frac{IR\omega L}{R^2 + (\omega L)^2} e^{-\frac{R(\omega t)}{\omega L}} - \frac{IR}{\sqrt{R^2 + (\omega L)^2}} \cos(\omega t + \psi) \qquad (2)$$

From Real Translation Theorem;

$$E_2(t) = \left[\frac{-IR^2\omega L}{R^2 + (\omega L)^2} e^{-\frac{R(\omega t - \pi)}{\omega L}} + \frac{\omega L IR}{\sqrt{R^2 + (\omega L)^2}} \sin(\omega t - \pi + \psi)\right] \cdot u(\omega t - \pi)$$

Therefore for $\pi \le \omega t$, define $\omega t' = \omega t - \pi$, and

$$e(t) = E_1(t) + E_2(t) = -\frac{IR^2\omega L}{R^2 + (\omega L)^2} e^{-\frac{R\omega t'}{\omega L}} \left[1 + e^{-\frac{R\pi}{\omega L}}\right] \qquad (1a)$$

$$i_m = -e(t)/R \qquad (2a)$$

2. DERIVATION OF EQUATIONS FOR PLOTTING FIGURE 14
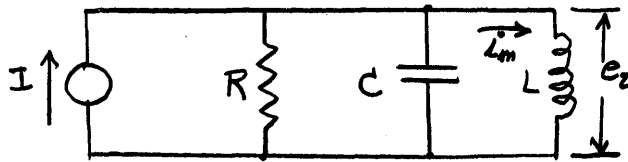
Figure B-3

In figure B-3 all values are referred to the secondary. From

the node equation in Laplace Transforms;

$$E(s) = \frac{sI(s)}{C\left(s^2 + \frac{s}{RC} + \frac{1}{LC}\right)} = \frac{sI\omega\left(1 + e^{-\frac{\pi}{\omega}s}\right)}{C\left(s^2 + \frac{s}{RC} + \frac{1}{LC}\right)(s^2 + \omega^2)} \triangleq E_1(s) + E_2(s)$$

The roots of the characteristic equation for the overdamped case are:

$$\alpha_1 \triangleq \frac{1}{2RC} - \sqrt{\frac{1}{(2RC)^2} - \frac{1}{LC}}$$

$$\alpha_2 \triangleq \frac{1}{2RC} + \sqrt{\frac{1}{(2RC)^2} - \frac{1}{LC}}$$

For $0 \leq \omega t \leq \pi$

$$E_1(s) = \frac{I}{C} \quad \frac{s\,\omega}{(s+\alpha_1)(s+\alpha_2)(s^2+\omega^2)}$$

Solving for the residues, the terminal voltage can be expressed as:

$$e_t = E_1(t) = \frac{I}{C}\left[K_1 e^{-\alpha_1 t} + K_2 e^{-\alpha_2 t} + \mathcal{J}\left(\frac{j\,\omega}{(\alpha_1 + j\,\omega)(\alpha_2 + j\omega)} e^{j\omega t}\right)\right] \quad (3)$$

where

$$K_1 = \frac{-\alpha_1 \omega}{(\alpha_2 - \alpha_1)(\omega^2 + \alpha_1^2)}$$

$$K_2 = \frac{\alpha_2 \omega}{(\alpha_2 - \alpha_1)(\omega^2 + \alpha_2^2)}$$

$$\mathcal{J}\left[\frac{j\,\omega}{(\alpha_1 + j\omega)(\alpha_2 + j\omega)} e^{j\omega t}\right] = \frac{\omega}{\sqrt{(\alpha_1^2 + \omega^2)(\alpha_2^2 + \omega^2)}} \sin(\omega t + \phi)$$

Since $I_m(s) = \dfrac{E_t(s)}{Ls}$,

$$i_m = \frac{I}{LC}\left[\frac{-K_1}{\alpha_1} e^{-\alpha_1 t} - \frac{K_2}{\alpha_2} e^{-\alpha_2 t} - \frac{1}{\sqrt{(\alpha_1^2 + \omega^2)(\alpha_2^2 + \omega^2)}} \cos(\omega t + \phi)\right] \quad (4)$$

For $\pi \leq \omega t$, define $\omega t' = \omega t - \pi$. Using the Real Translation Theorem and combining terms:

$$e_t = E_1(t) + E_2(t)$$

$$= \frac{I}{C}\left[K_1 e^{-\alpha_1 t'}(1 + e^{-\alpha_1 \frac{\pi}{\omega}}) + K_2 e^{-\alpha_2 t'}(1 + e^{-\alpha_2 \frac{\pi}{\omega}})\right] \quad (3a)$$

$$i_m = \frac{I}{LC}\left[\frac{-K_1}{\alpha_1} e^{-\alpha_1 t'}(1 + e^{-\alpha_1 \frac{\pi}{\omega}}) - \frac{K_2}{\alpha_2} e^{-\alpha_2 t'}(1 + e^{-\alpha_2 \frac{\pi}{\omega}})\right] \quad (4a)$$

3. DERIVATION OF EQUATIONS FOR PLOTTING FIGURE 15
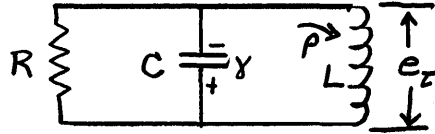
Figure B-4

The conditions for Figure 14 for R = 93 ohms, C = 90 mmf, and L = 9.4 microhenries are assumed to exist for $0 \leq \omega t \leq \pi$. At $\omega t = \pi$ a current ρ exists in the inductance and a charge γ across the condenser as shown in Figure B-4. The inductance L is now allowed to change to $L' = \frac{1}{2}L = 4.7$ microhenries. From the node equations in Laplace Transforms:

$$E(s) = \frac{-\rho + \gamma Cs}{C\left(s^2 + \frac{s}{RC} + \frac{1}{L'C}\right)} = \frac{-\rho + \gamma Cs}{C(s + \alpha_1')(s + \alpha_2')}$$

where

$$\alpha_1' \triangleq \frac{1}{2RC} - \sqrt{\left(\frac{1}{2RC}\right)^2 - \frac{1}{L'C}}$$

$$\alpha_2' \triangleq \frac{1}{2RC} + \sqrt{\left(\frac{1}{2RC}\right)^2 - \frac{1}{L'C}}$$

The inverse transform is:

$$e_t = K_1' e^{-\alpha_1' t'} + K_2' e^{-\alpha_2' t'} \tag{5}$$

where

$$K_1' = \frac{(-\rho + \gamma C\alpha_1')}{C(\alpha_2' - \alpha_1')}$$

$$K_2' = \frac{(\rho + \gamma C\alpha_2')}{C(\alpha_2' - \alpha_1')}$$

$$\omega t' = \omega t - \pi$$

Similarly,

$$i_m = \frac{1}{L}\left(\frac{-K_1'}{\alpha_1'} e^{-\alpha_1' t'} - \frac{K_2'}{\alpha_2'} e^{-\alpha_2' t'}\right) \tag{6}$$

4. DEVELOPMENT OF DESIGN FORMULAE FOR 3:1 PULSE TRANSFORMERS

Inductance L is defined as flux linkages per ampere:*

$$L = \frac{\phi N}{i_m} \times 10^{-8} = \frac{BAN}{i_m} \times 10^{-8} \text{ henries}$$

where

N = number of turns

A = cross sectional area (cm^2)

i_m = magnetizing current (amperes)

B = flux density (gauss)

From $\Delta B = \mu_\epsilon \Delta H$, where μ_ϵ is the effective pulse permeability, and

$$H = \frac{0.4 \pi N i_m}{l_m} \text{ oersteds}$$

where l_m = mean magnetic path length (cm),

$$L = \frac{0.4 \pi N^2 A \mu_\epsilon}{l_m} 10^{-8}$$

or

$$N = \sqrt{\frac{L l_m 10^8}{0.4 \pi A \mu_\epsilon}} \tag{7}$$

The flux density required to sustain a pure half-sine of voltage

across the terminals of a transformer is derived as follows:

$$e_t = NA \frac{dB}{dt} 10^{-8} = E_t \sin \omega t \quad \text{(volts)} \quad, \text{ for } 0 \leq \omega t \leq \pi$$

$$\Delta B_{max} = \frac{10^8}{NA} \int_0^\pi \frac{E_t}{\omega} \sin \omega t \, d(\omega t) = \frac{2 E_t}{NA \omega} 10^8$$

Since $\omega = 2 \pi f = \frac{\pi}{T}$, where T = pulse length in seconds,

$$\Delta B_{max} = \frac{2 E_t}{\pi NA} T 10^8 \tag{8}$$

* Reuben Lee: <u>Electronic Transformers and Circuits</u>, John Wiley & Sons,
1947. p. 75

APPENDIX C

1:1 PULSE TRANSFORMER EQUATIONS

1. ALGEBRAIC SOLUTION FOR FINDING THE NATURAL FREQUENCIES OF THE

   1:1 PULSE TRANSFORMER EQUIVALENT CIRCUIT

From Figure 17 and using the complex frequency "s":

$$T(s) = \frac{E_2}{V}(s) = \frac{Y_1}{Y_1 + Y_2}$$

Since

$$Y_1(s) = \frac{1}{\frac{1}{sC_1} + s\ell} \quad , \qquad Y_2(s) = sC_2 + \frac{1}{sL}$$

$$T(s) = \frac{1}{\ell C_2}\left[\frac{s^2}{s^4 + s^2\left(\frac{1}{\ell C_2} + \frac{1}{\ell C_1} + \frac{1}{LC_2}\right) + \frac{1}{LC_1C_2}}\right] \quad (9)$$

Let $\omega_1^2 = \frac{1}{\ell C_1}$, $\omega_2^2 = \frac{1}{LC_2}$

Since $\sigma = \frac{\ell}{L + \ell}$ *,

the denominator of T(s) may be written:

$$s^4 + s^2\left(\frac{\omega_2^2}{\sigma} + \omega_1^2\right) + \omega_1^2 \omega_2^2$$

Let

$$\alpha = \frac{\frac{\omega_2^2}{\sigma} + \omega_1^2}{2} \quad (10)$$

and

$$\beta = \omega_1^2 \omega_2^2 \quad (11)$$

Then the roots of the denominator of T(s) become:

$$s^2 = -\alpha \pm \sqrt{\alpha^2 - \beta}$$

---

* This results from the fact that in Fig. 16, $\ell = L_1\sigma$, and $L = L_1(1-\sigma)$

The natural frequencies of Figure 17 can thus be expressed by:

$$\omega_R{}'' = \sqrt{\alpha + \sqrt{\alpha^2 - \beta}} \qquad (12)$$

$$\omega_R{}' = \sqrt{\alpha - \sqrt{\alpha^2 - \beta}} \qquad (13)$$

2. THE SOLUTION FOR THE RESPONSE OF THE 1:1 PULSE TRANSFORMER TO A

HALF-SINE CURRENT PULSE SOURCE

Expressing (9) in terms of natural frequencies:

$$T(s) = \frac{E_2}{V}(s) = \frac{1}{\ell C_2} \cdot \left[\frac{s^2}{(s^2 + \omega_R'^2)(s^2 + \omega_R''^2)} \right]$$

Since $V(s) = \frac{I(s)}{C_1 s}$,

$$E_2(s) = \frac{1}{\ell C_1 C_2} \left[\frac{s\, I(s)}{(s^2 + \omega_R'^2)(s^2 + \omega_R''^2)} \right]$$

For a half-sine current pulse in the Laplace Transforms:

$$I(s) = \frac{I\,\omega}{(s^2 + \omega^2)} (1 + e^{-\frac{\pi}{\omega}s}) \triangleq I_1(s) + I_2(s)$$

For $0 \doteq \omega t \doteq \pi$,

$$E_2(s) = \frac{I\,\omega}{\ell C_1 C_2} \left[\frac{s}{(s^2 + \omega_R'^2)(s^2 + \omega_R''^2)(s^2 + \omega^2)} \right]$$

Evaluating residues and expressing in the time domain:

$$E_2(t) = IK \left[\frac{\cos y\,\omega t}{(x^2 - y^2)(1 - y^2)} + \frac{\cos x\,\omega t}{(x^2 - y^2)(x^2 - 1)} - \frac{\cos \omega t}{(x^2 - 1)(1 - y^2)} \right] \qquad (14)$$

where

$$K = \frac{1}{\ell C_1 C_2}\,\omega^3 \qquad (15)$$

$$x = \omega_R''/\omega \qquad (16)$$

$$y = \omega_R'/\omega \qquad (17)$$

For $\pi \leq \omega t$

$$E_2(t) = KI \left[\frac{\cos y \omega t + \cos y(\omega t - \pi)}{(x^2-y^2)(1-y^2)} + \frac{\cos x \omega t + \cos x(\omega t - \pi)}{(x^2-y^2)(x^2-1)} \right] \quad (18)$$

The units for all expressions are:

C_1 and C_2 in farads

L and ℓ in henries

I in amperes

E_2 and V in volts

t in seconds
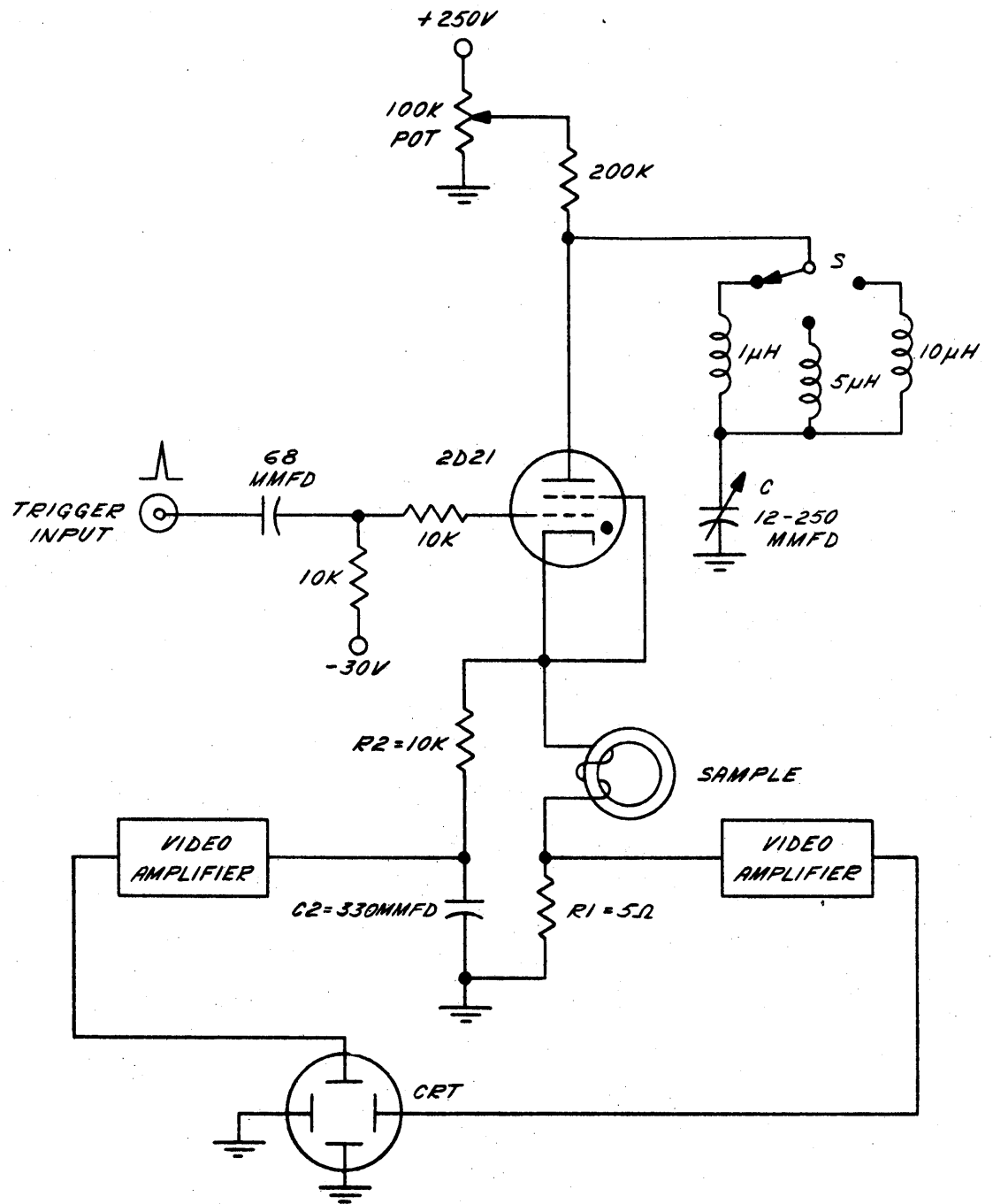
FIG. 1

APPARATUS FOR TAKING PULSE HYSTERESIS LOOPS

A-51976
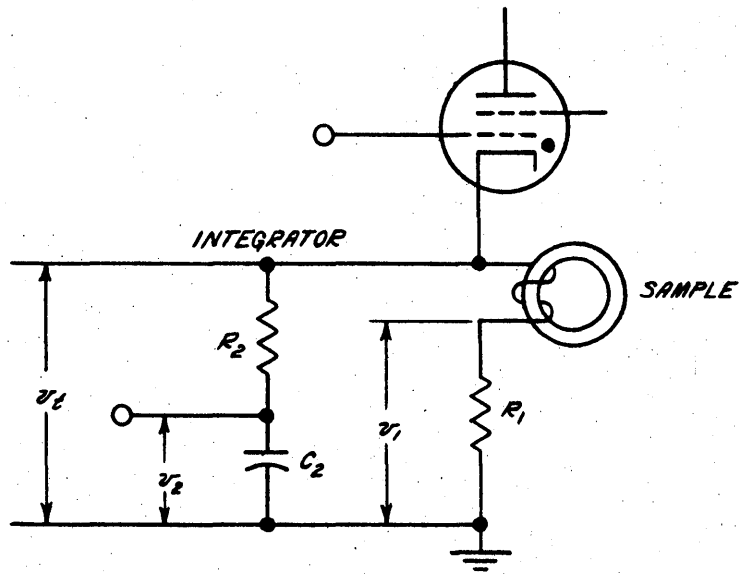
TEST CIRCUIT
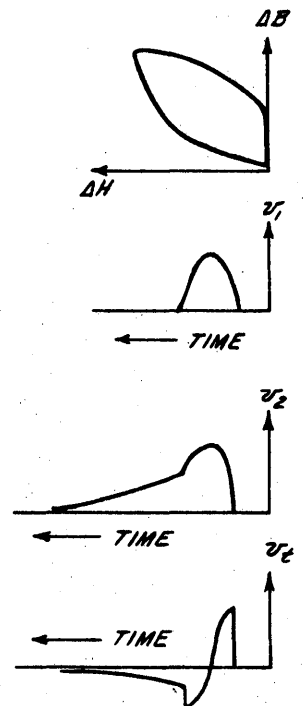
VOLTAGE WAVE SHAPES
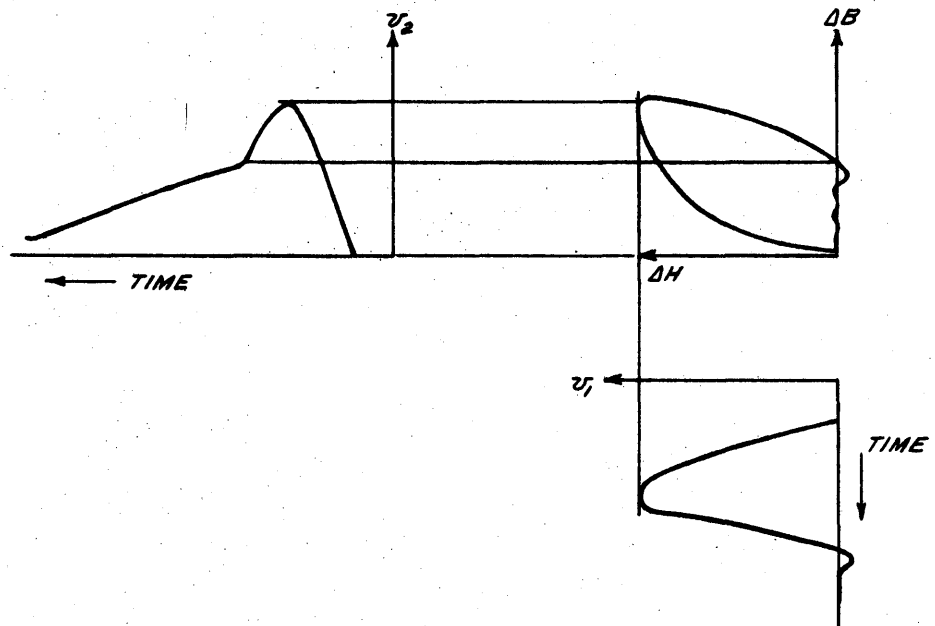
HOW THE PULSE LOOP IS FORMED

FIG. 2

PULSE HYSTERESIS LOOPS
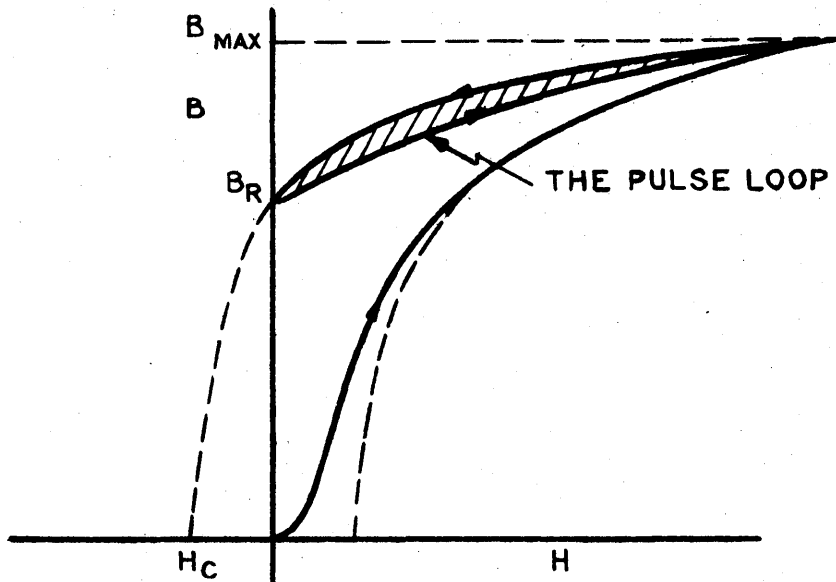
FORMATION OF A D-C "PULSE" LOOP
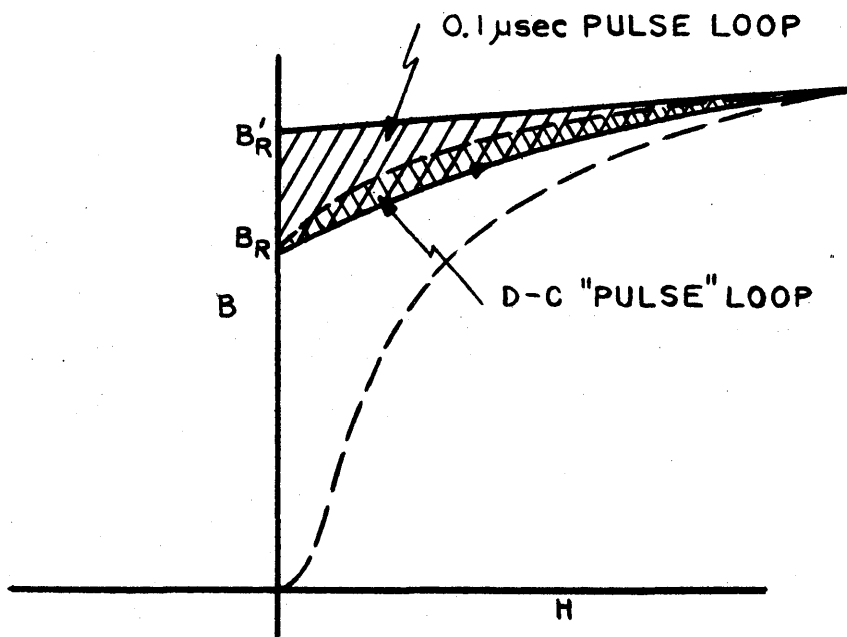
FIG. 3

THE FAST PULSE DOES NOT FOLLOW THE
SAME PATH AS THE D-C "PULSE"
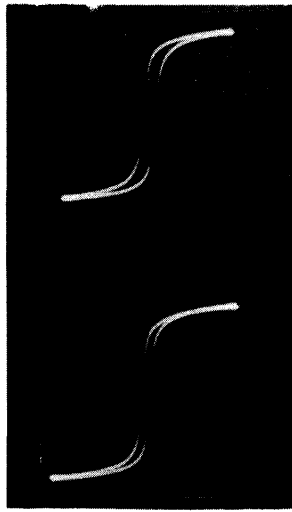
FERRAMIC H
Hmax = 4 OERSTEDS
Hmax = 8 OERSTEDS
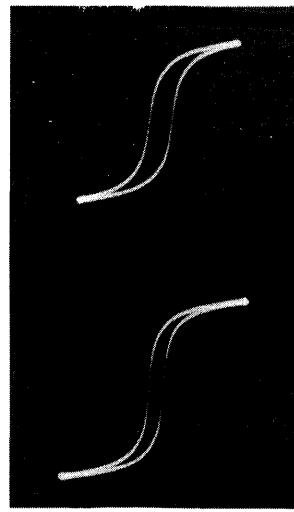
CERAMAG 5N
Hmax = 4 OERSTEDS
Hmax = 8 OERSTEDS
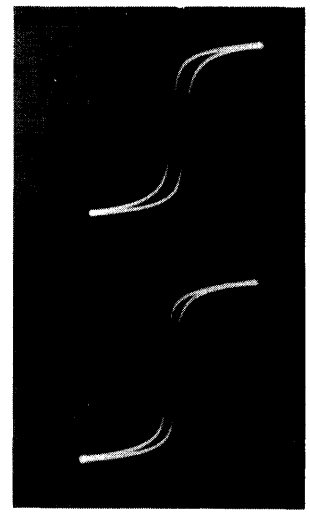
CERAMAG 7A
Hmax = 4 OERSTEDS
Hmax = 8 OERSTEDS
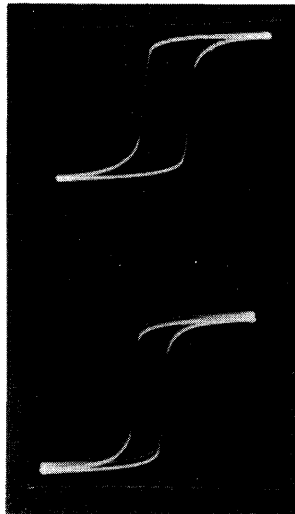
MF 1131
Hmax = 4.8 OERSTEDS
Hmax = 8.3 OERSTEDS
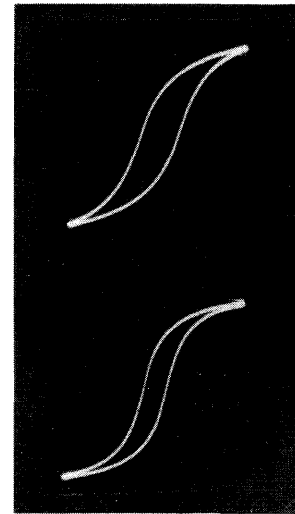
FERRICORE
Hmax = 4 OERSTEDS
Hmax = 8 OERSTEDS

FIG. 4

60-CYCLE HYSTERESIS LOOPS
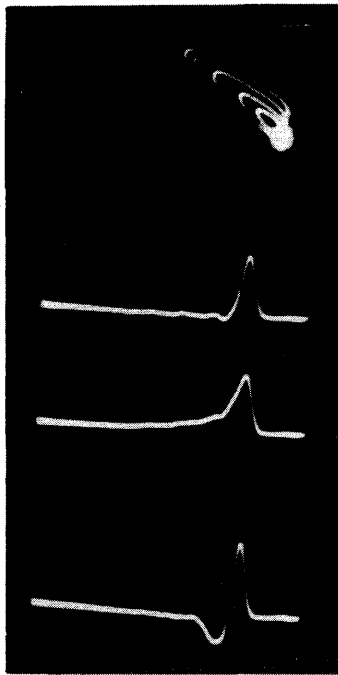
FERRAMIC H
PULSE LENGTH 0.1 μSEC
ΔBmax = 475 GAUSS
ΔHmax = 1.22 OERSTEDS
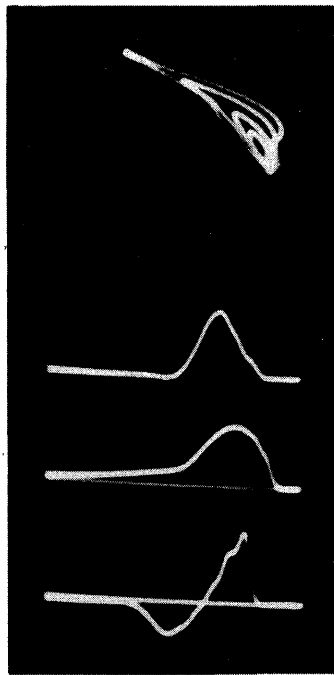
FERRAMIC H
PULSE LENGTH 0.3 μSEC
ΔBmax = 1660 GAUSS
ΔHmax = 9.1 OERSTEDS
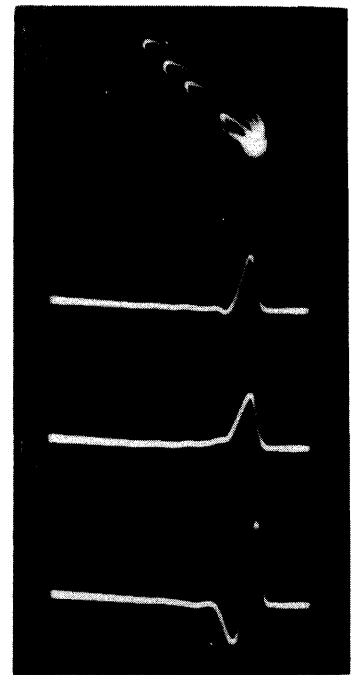
CERAMAG 5N
PULSE LENGTH 0.1 μSEC
ΔBmax = 570 GAUSS
ΔHmax = 1.69 OERSTEDS
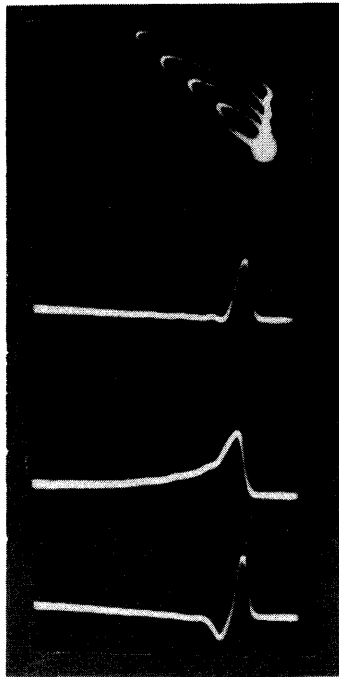
CERAMAG 7A
PULSE LENGTH 0.1 μSEC
ΔBmax = 700 GAUSS
ΔHmax = 2.31 OERSTEDS
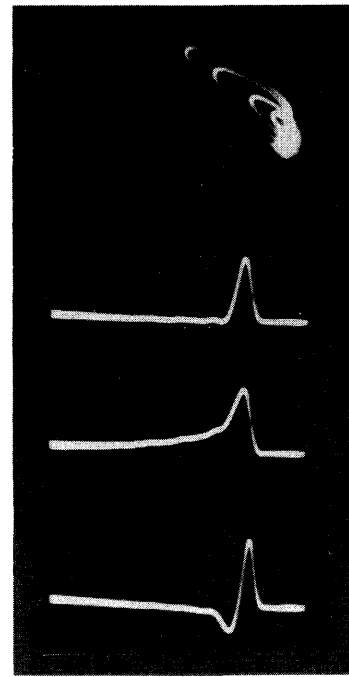
I MIL HYPERSIL
PULSE LENGTH 0.1 μSEC
ΔBmax = 91 GAUSS
ΔHmax = 0.84 OERSTEDS

FIG. 5

PULSE HYSTERESIS LOOPS
OF DIFFERENT MATERIALS
PART I
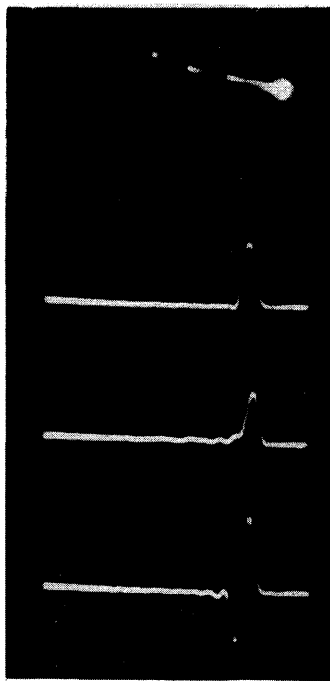
MF 1131
PULSE LENGTH 0.1 μSEC
Δ Bmax = 250 GAUSS
Δ Hmax = 3.29 OERSTEDS
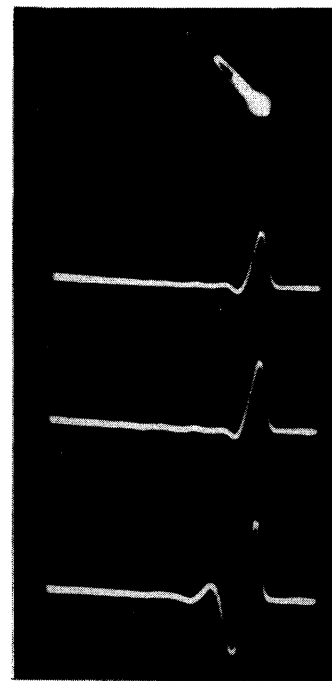
FERRICORE
PULSE LENGTH 0.1 μSEC
Δ Bmax = 367 GAUSS
Δ Hmax = 0.96 OERSTEDS
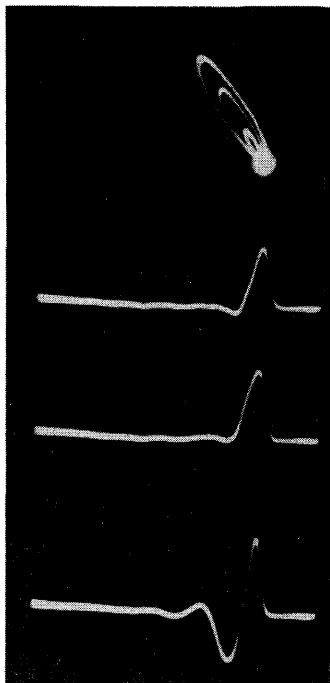
FERROXCUBE 3C
PULSE LENGTH 0.1 μSEC
Δ Bmax = 306 GAUSS
Δ Hmax = 0.64 OERSTEDS
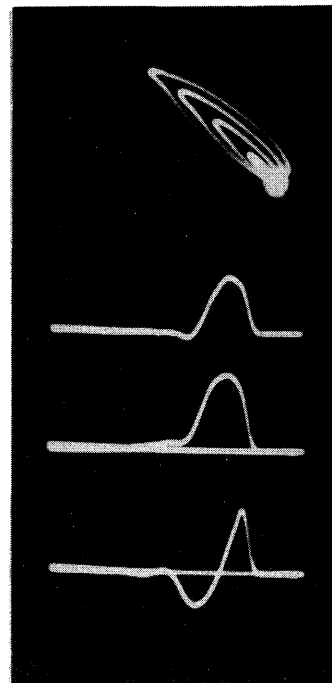
FERROXCUBE 3C
PULSE LENGTH 0.2 μSEC
Δ Bmax = 865 GAUSS
Δ Hmax = 1.73 OERSTEDS

FIG. 6

PULSE HYSTERESIS LOOPS
OF DIFFERENT MATERIALS
PART II
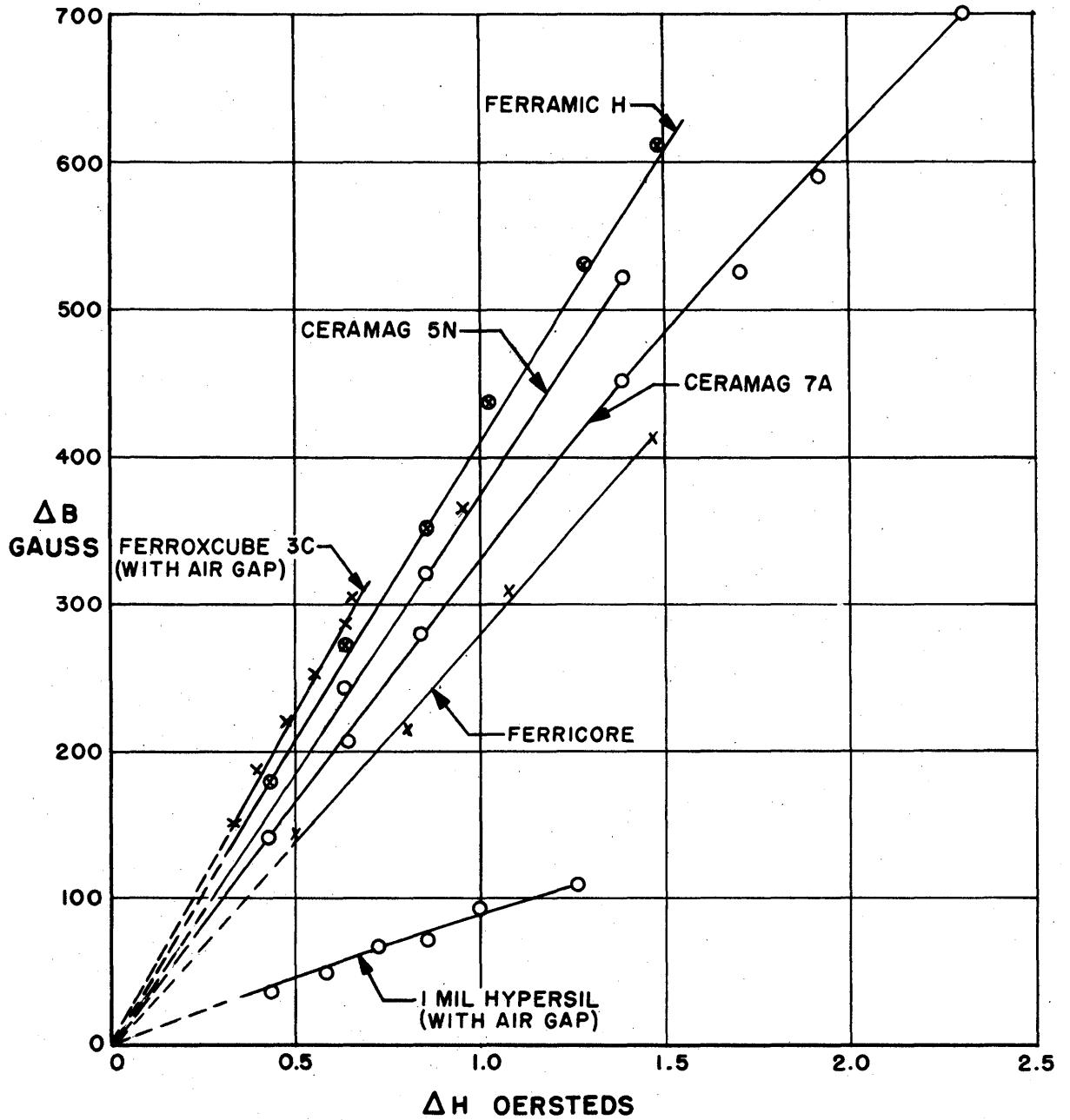
FIG. 7

PULSE MAGNETIZATION RESPONSE
PULSE SHAPE—0.1 MICROSECOND HALF—SINE
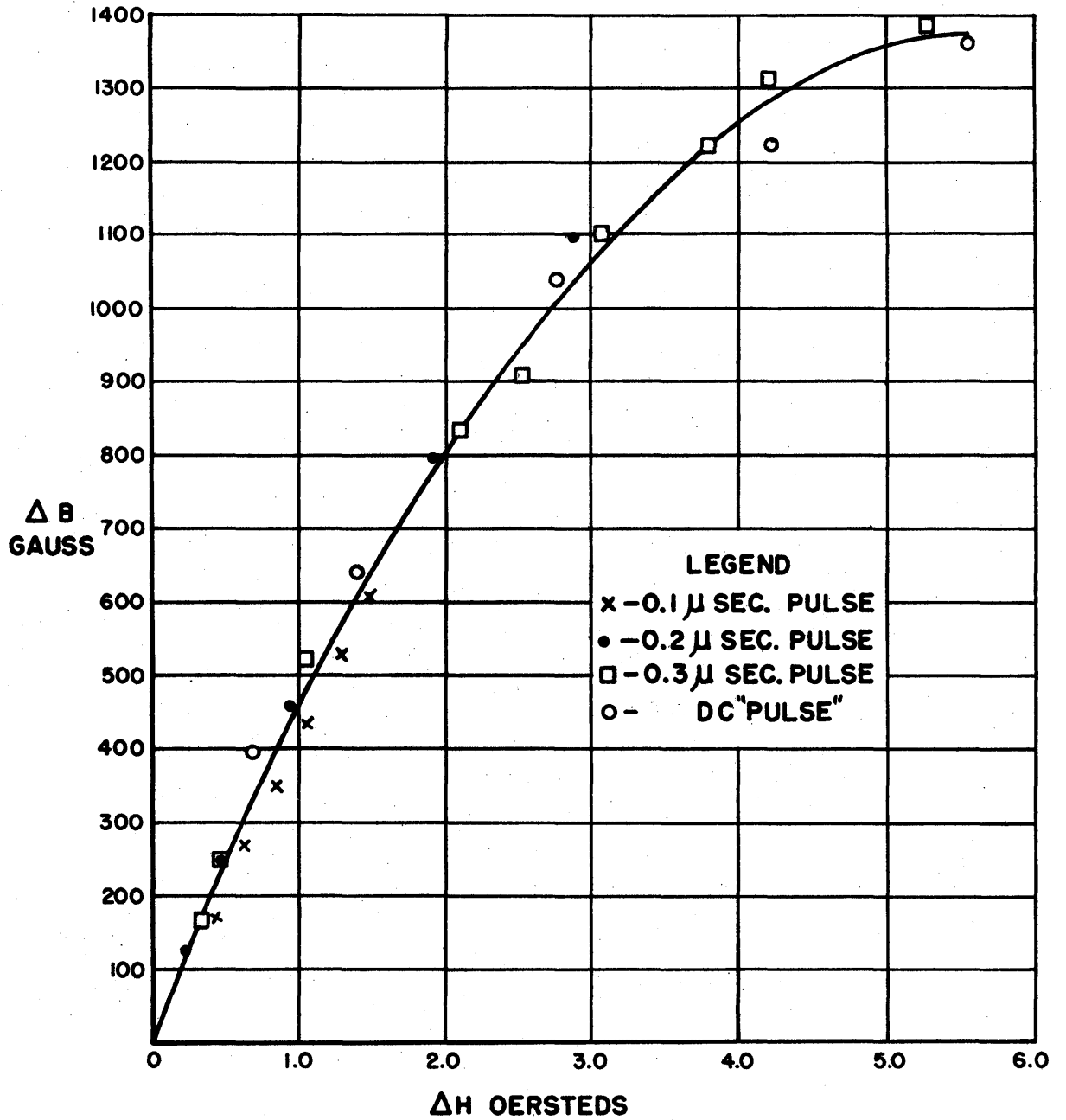
FIG. 8

PULSE MAGNETIZATION RESPONSE
CORRELATION OF SHORT AND LONG
TIME PULSE RESPONSE FOR FERRAMIC H

A-51974
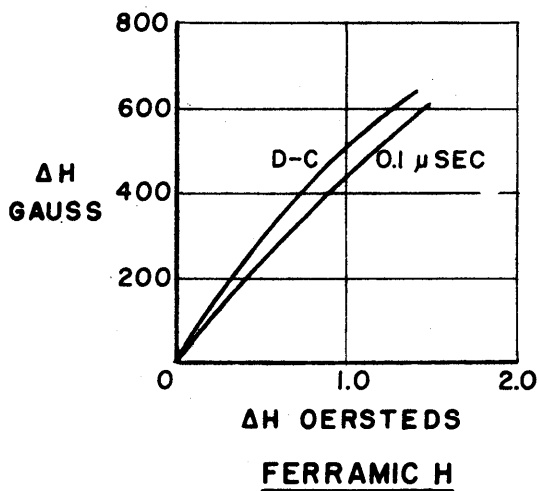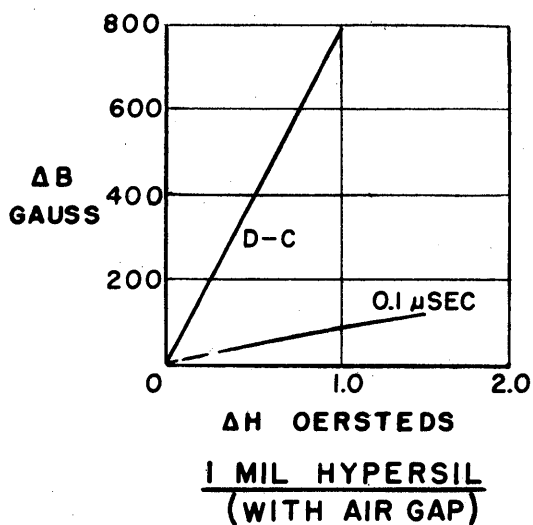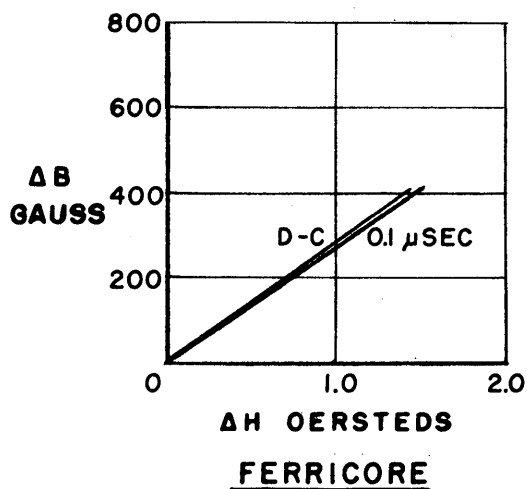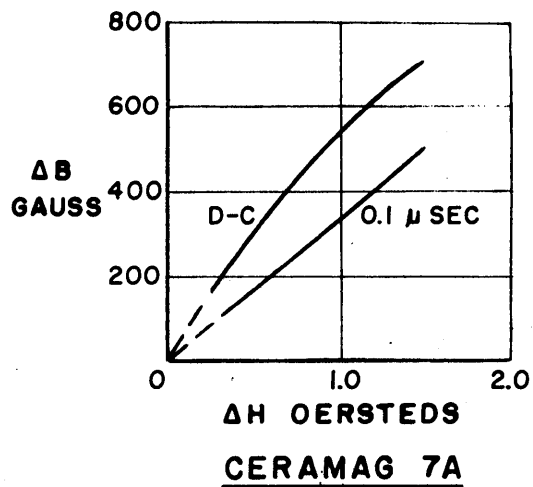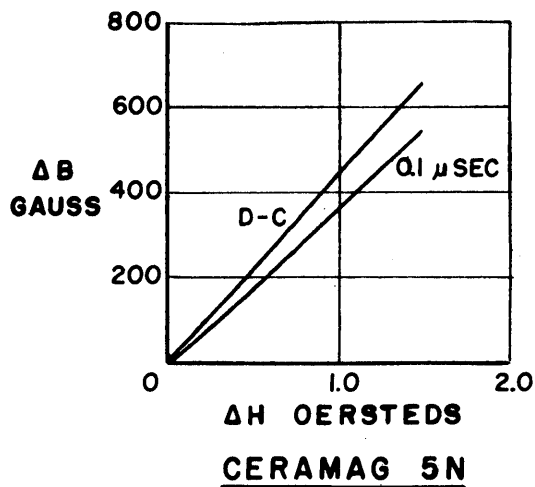
FIG. 9

PULSE MAGNETIZATION RESPONSE
OF VARIOUS MATERIALS FOR DC AND 0.1 μSEC PULSES
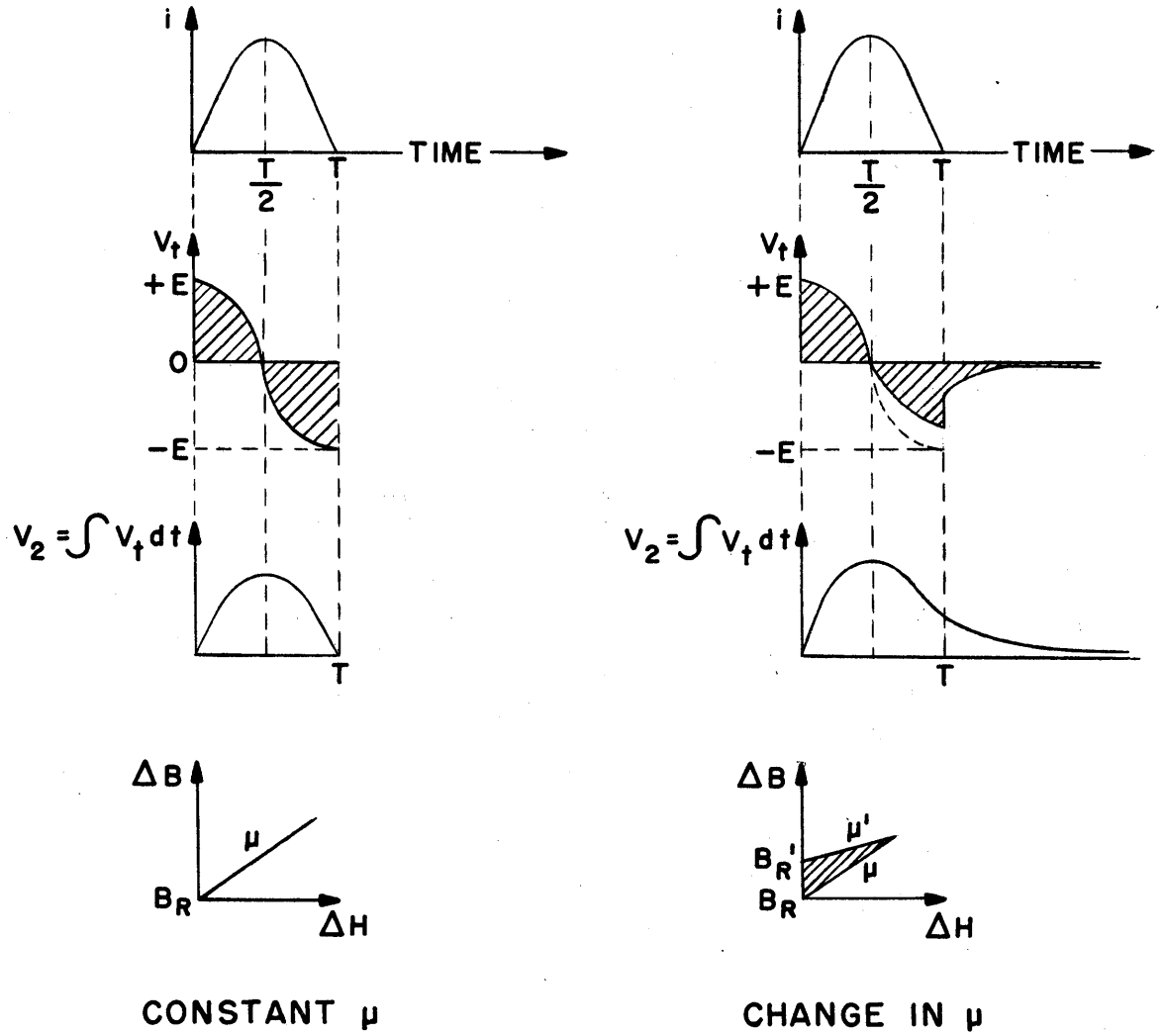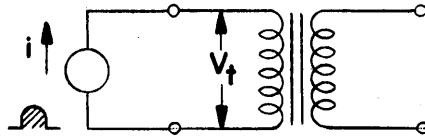
FIG. 10

OPEN—CIRCUITED TRANSFORMER WAVESHAPES

A-52046
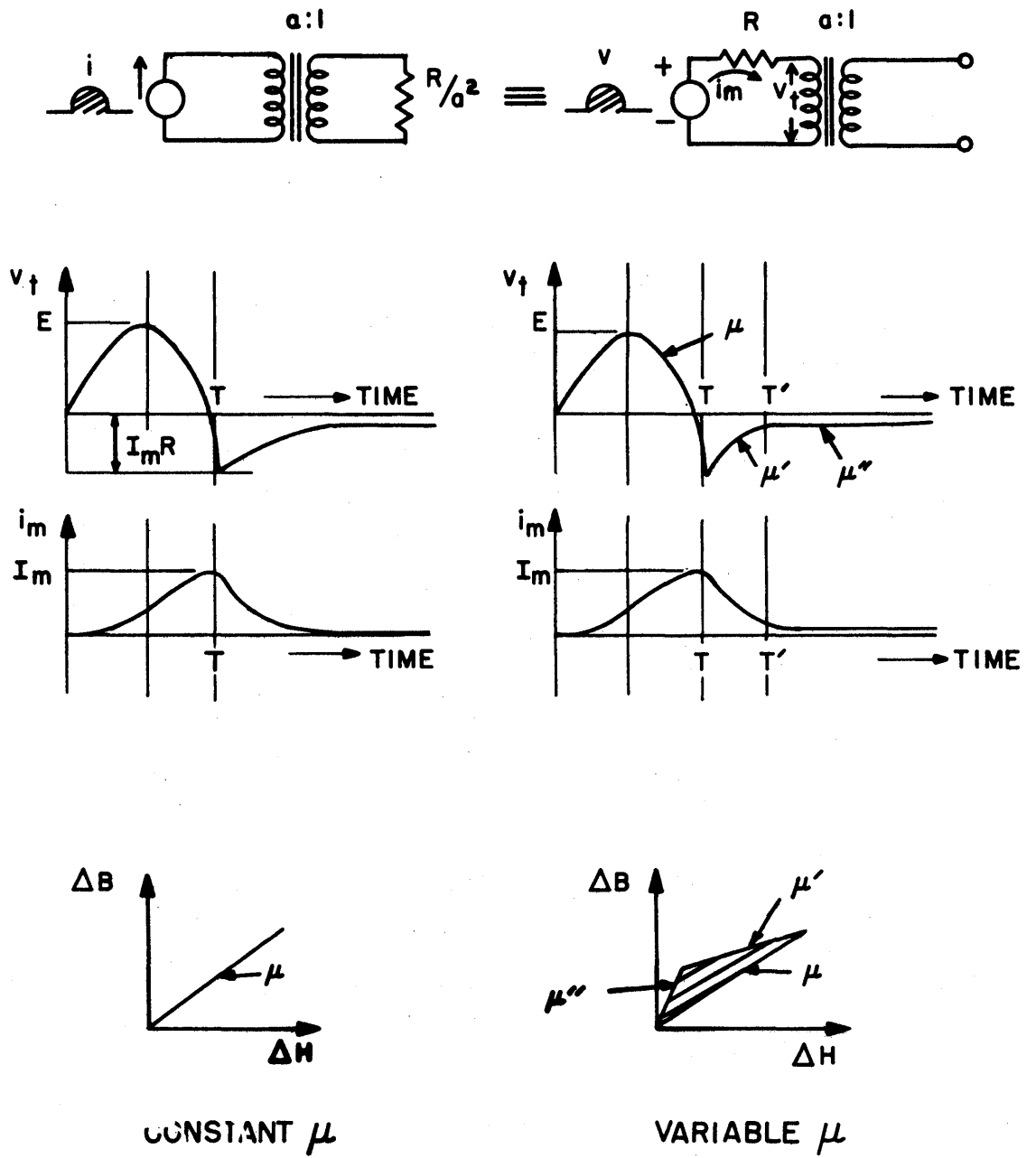
FIG. 11

VOLTAGE WAVESHAPES OF BASIC TRANSFORMER
WITH LOAD

GENERAL EQUIVALENT CIRCUIT
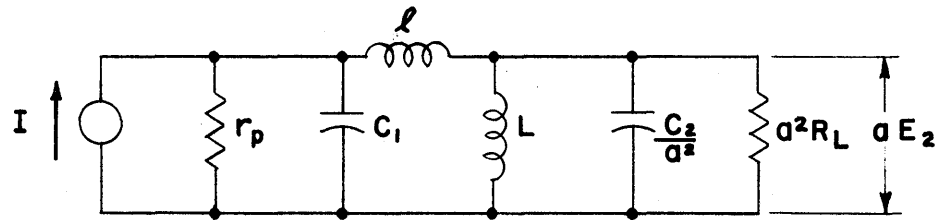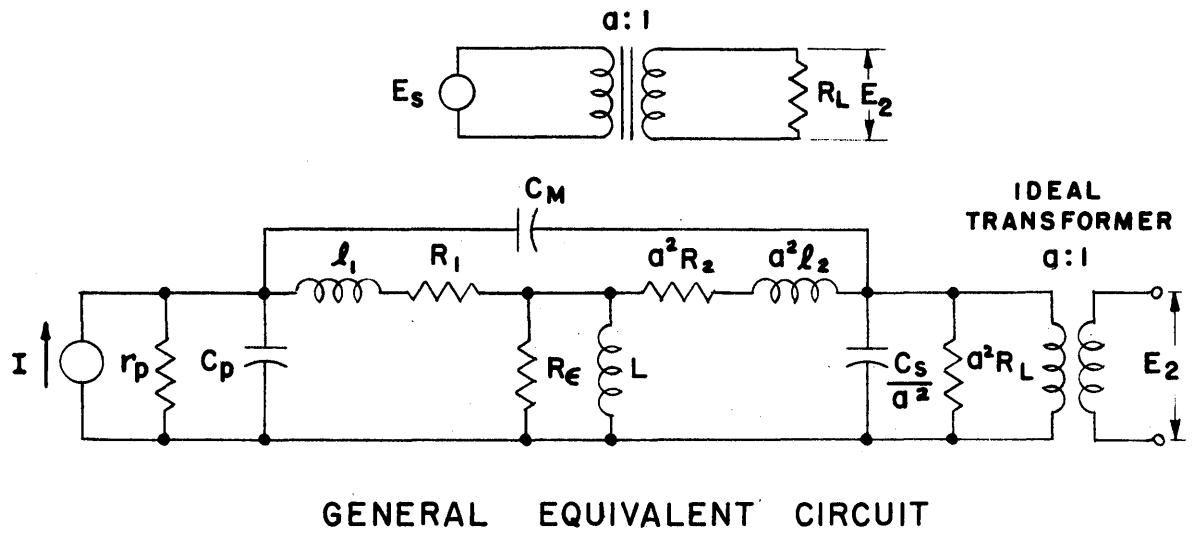
REDUCING NUMBER OF PARAMETERS
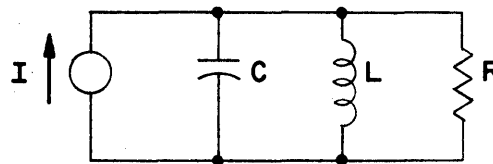
CIRCUIT FOR 3:1 TRANSFORMERS

FIG. 12

DEVELOPMENT OF 3:1 PULSE TRANSFORMER
EQUIVALENT CIRCUIT
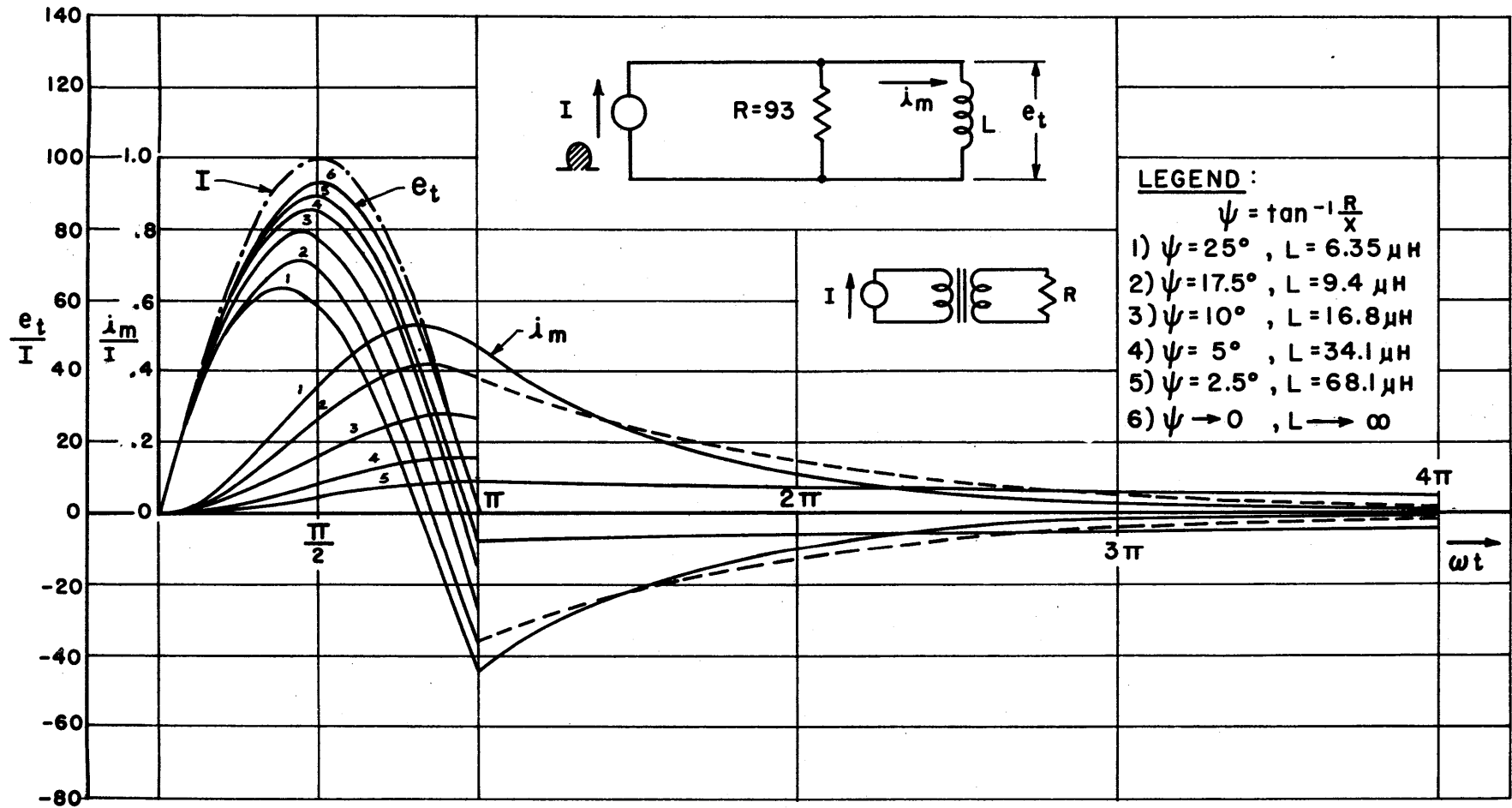
FIG. 13

WAVESHAPES OF BASIC TRANSFORMER WITH LOAD
AND WITH FINITE CONSTANT PERMEABILITY

A-52130
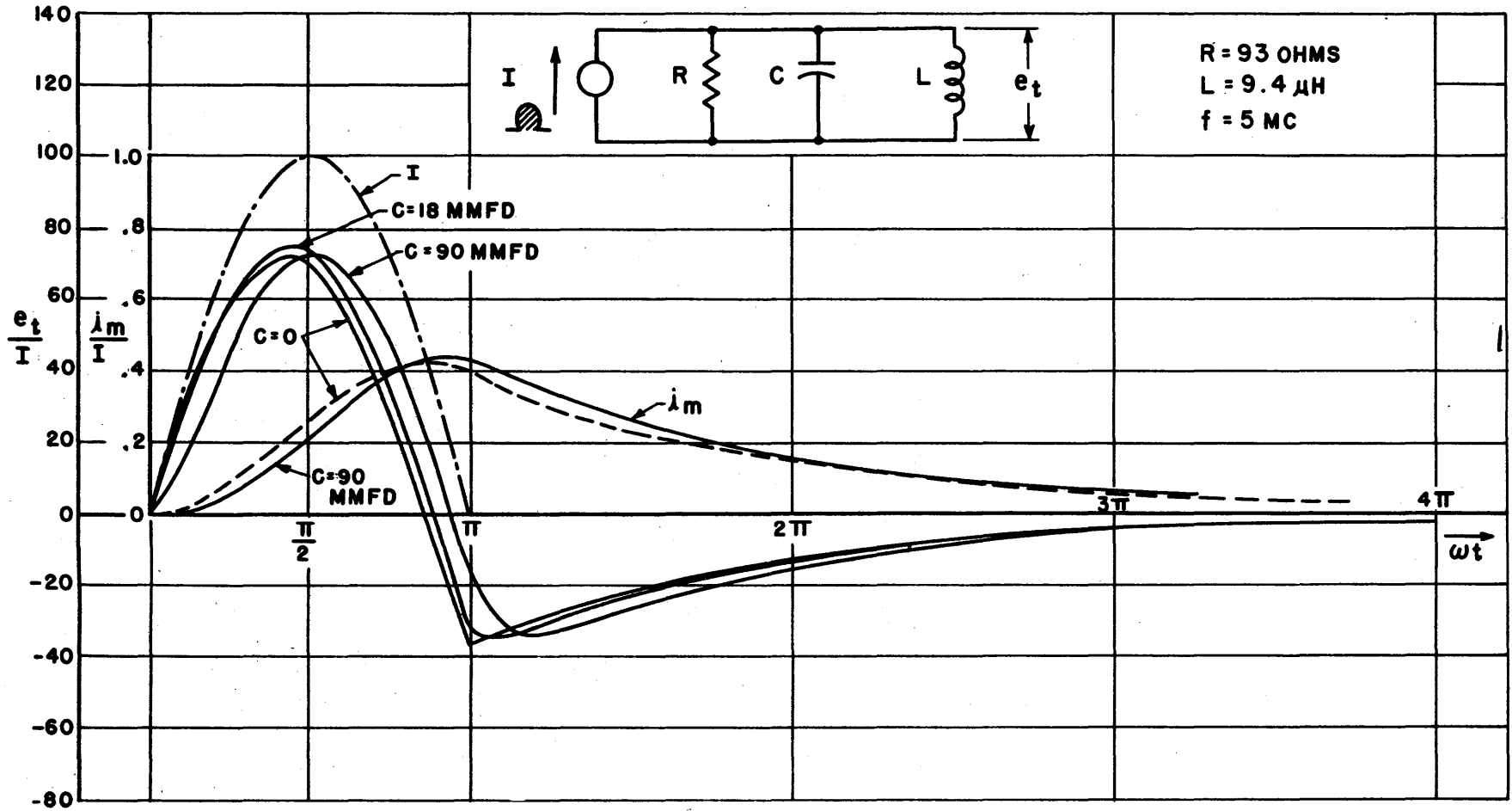
FIG. 14

EFFECT OF CAPACITANCES ON
TRANSFORMER WAVESHAPES
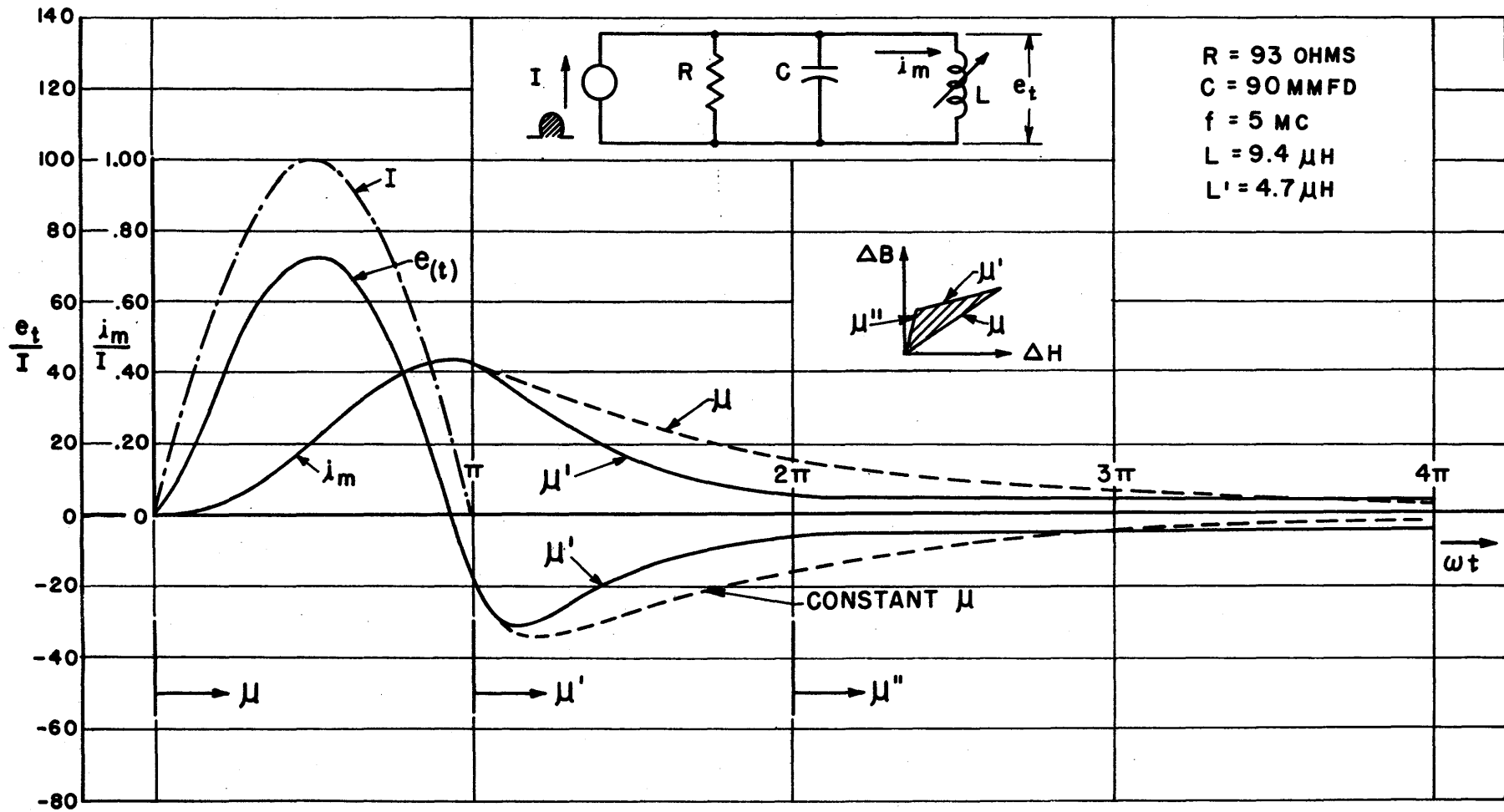
FIG. 15

EFFECT OF PERMEABILITY CHANGE
ON OVERSHOOT WAVESHAPE
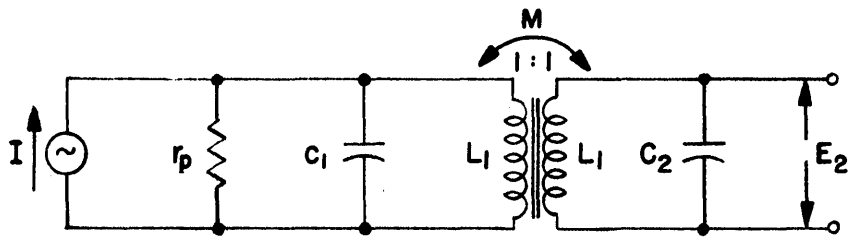
THE COUPLED CIRCUIT
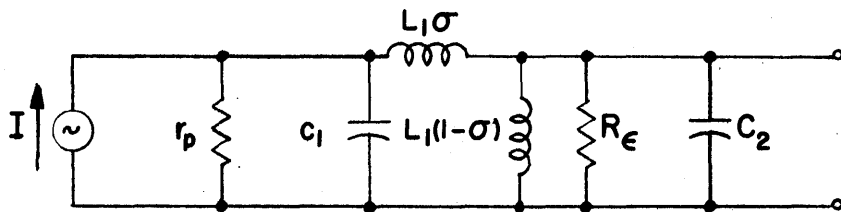
THE TRANSFORMER EQUIVALENT
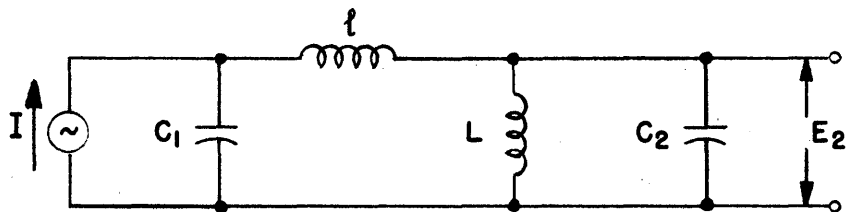
NEGLECTING RESISTANCES
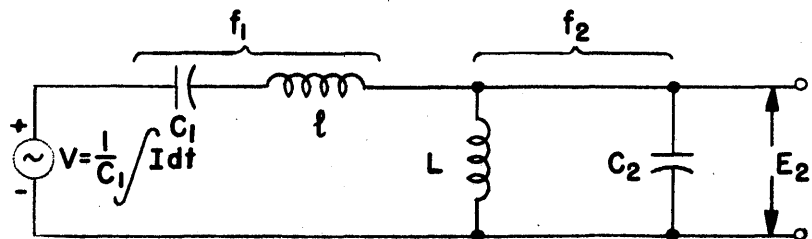
WITH AN EQUIVALENT VOLTAGE SOURCE

FIG. 16

DEVELOPMENT OF 1:1 PULSE TRANSFORMER
EQUIVALENT CIRCUIT
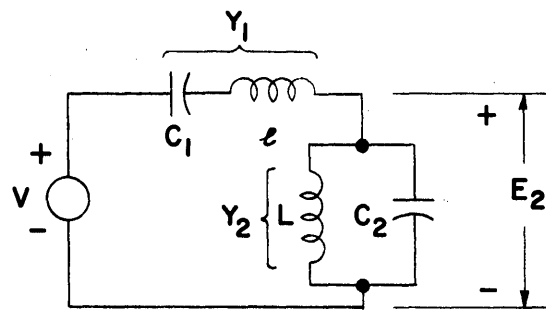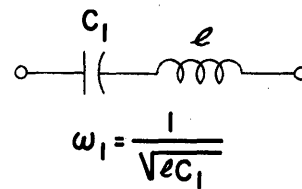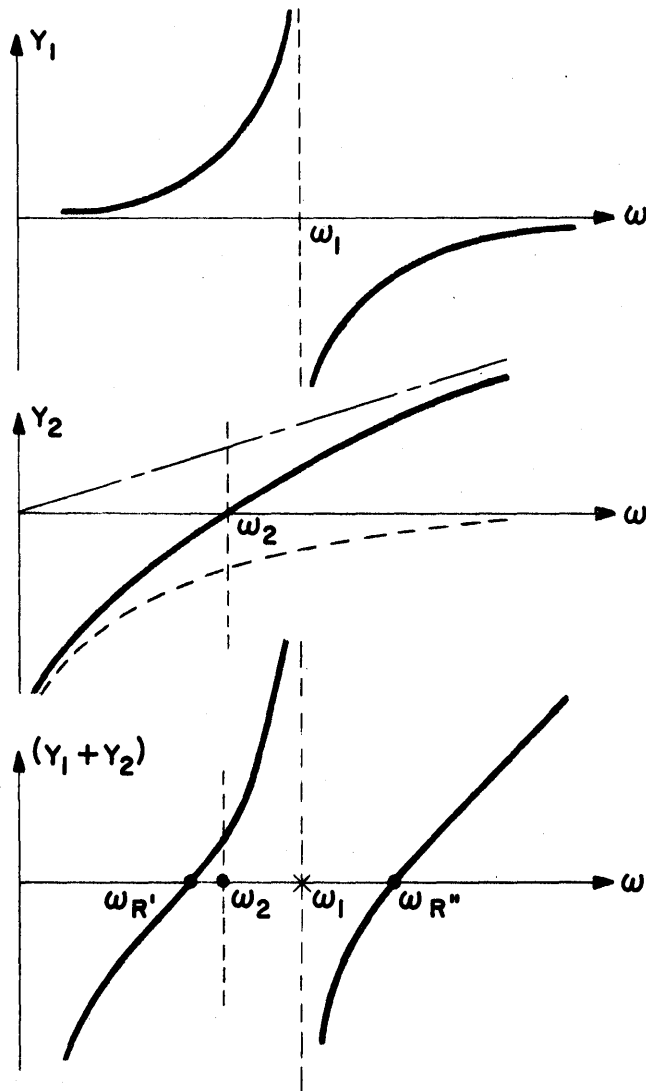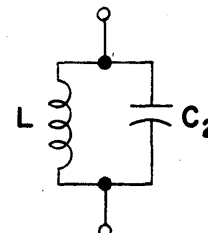
FIG. 17

SUSCEPTANCE PLOTS FOR LOCATING OSCILLATION
FREQUENCIES IN 1:1 TRANSFORMER
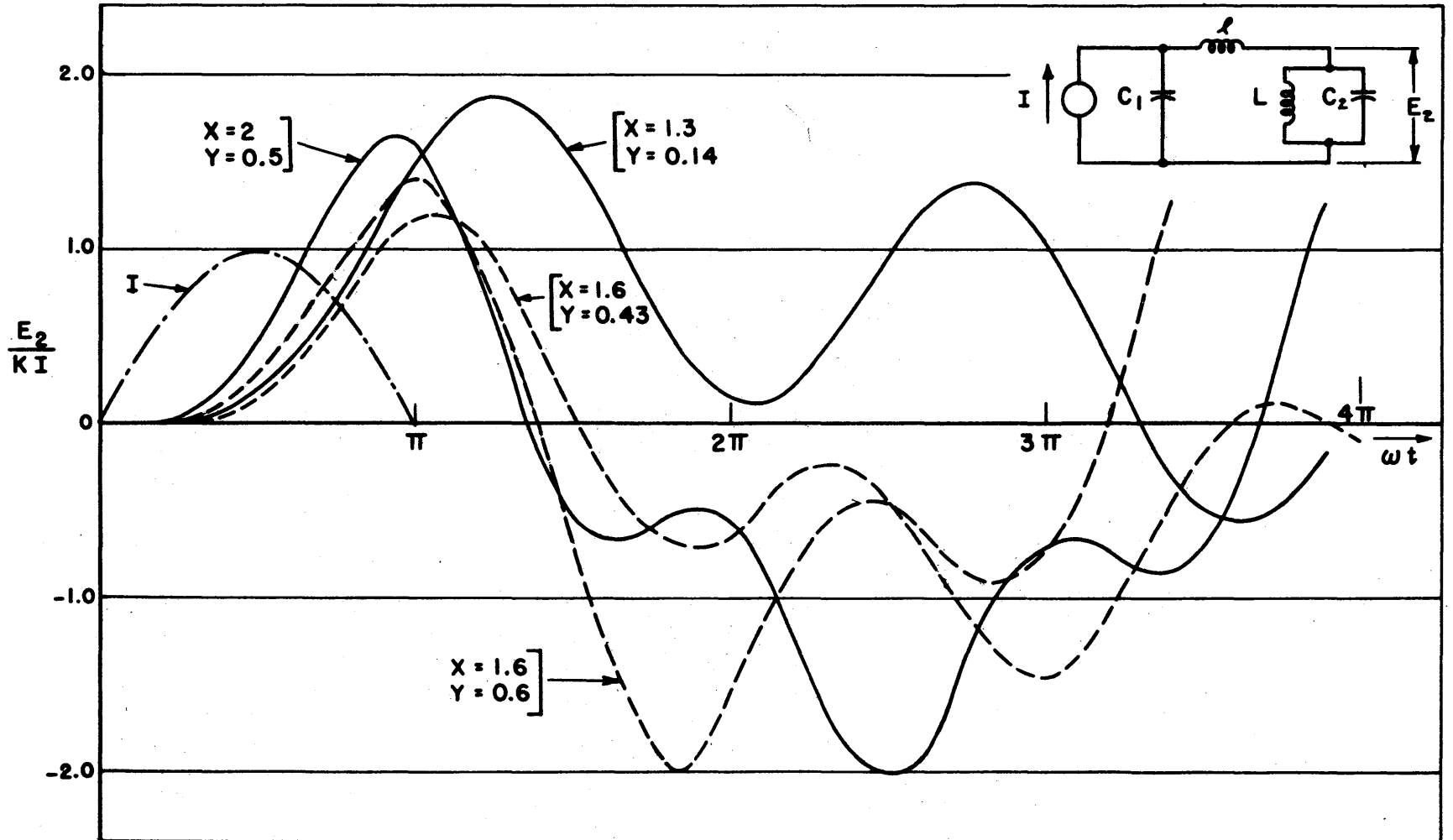
FIG 18 A

CALCULATED RESPONSE FROM EQUIVALENT
CIRCUIT OF 1:1 PULSE TRANSFORMER
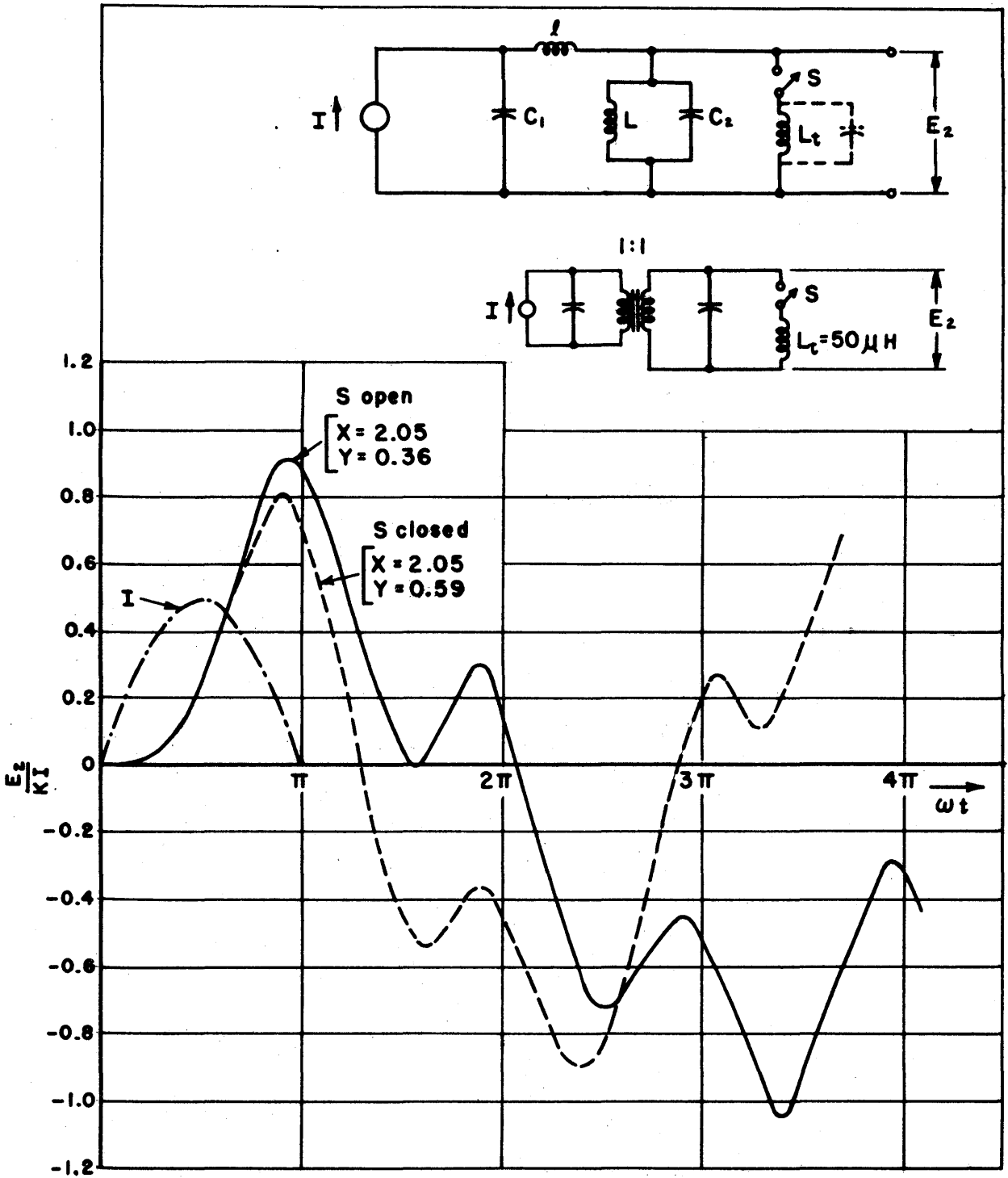
FIG. 18 B

CALCULATED RESPONSE OF 1:1 PULSE TRANSFORMER
WITH FERRITE CORE
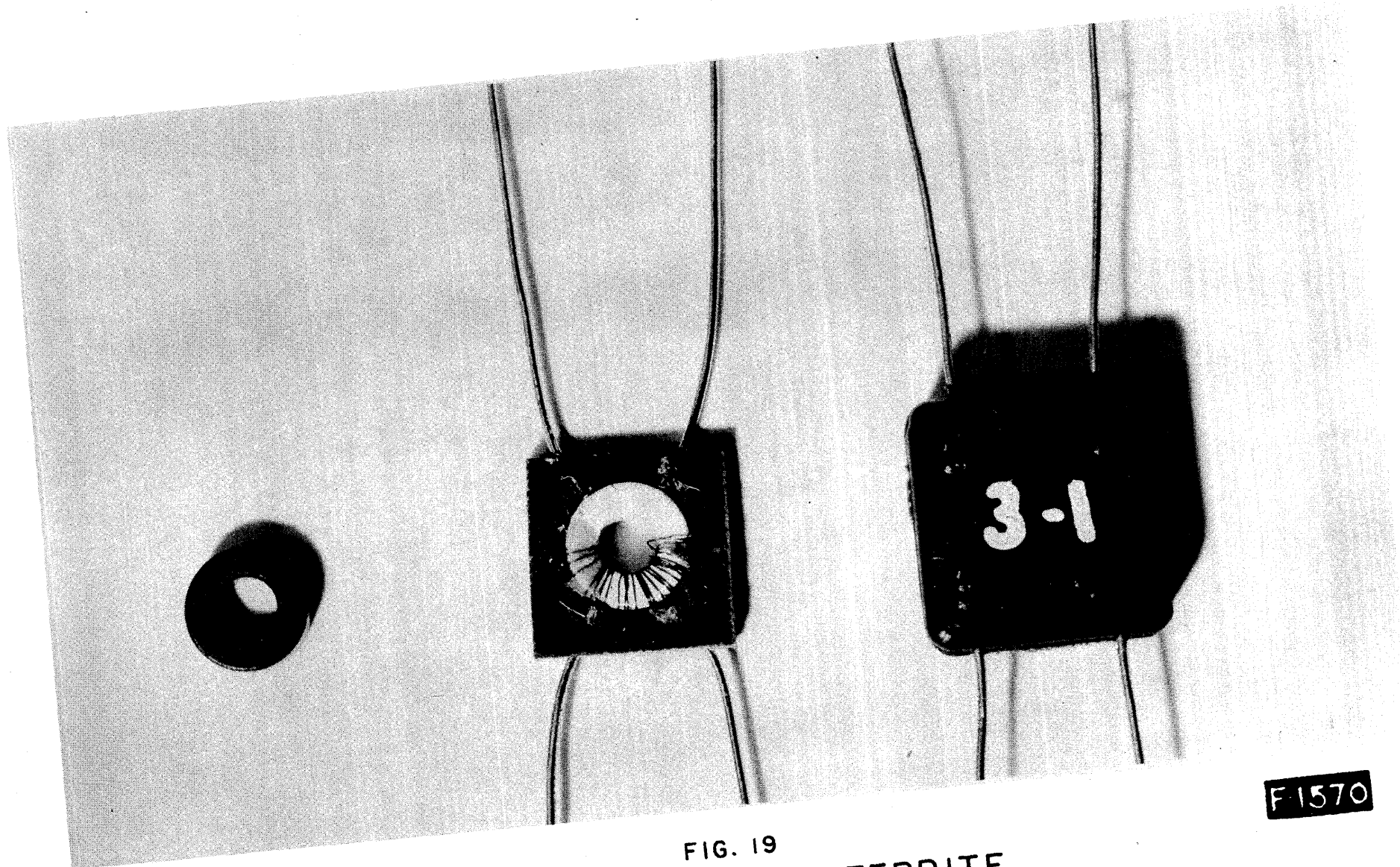
FIG. 19
CONSTRUCTION OF FERRITE
3:1 PULSE TRANSFORMER

+150V

S

470Ω   IN34

0.001 MFD

INPUT

7AK7

IN34

0.01 MFD

-15V

1:1

OUTPUT

S

L=50uH

+90V

1:1 PULSE TRANSFORMER
BASIC GATE TUBE CIRCUIT
(SUPPRESSOR GROUNDED TO CATHODE)

+250V

S

390Ω   IN34

0.001 MFD

INPUT

7AD7

IN34

15Ω

0.01 MFD

-15V

3:1

OUTPUT

+250V

3:1 PULSE TRANSFORMER
BASIC POINT-TO-POINT AMPLIFIER CIRCUIT

+150V

S

180Ω   IN34

0.01 MFD

INPUT

6Y6

2200Ω

0.01 MFD

-30V

5:1

OUTPUT

+150V

5:1 PULSE TRANSFORMER
GATE GENERATOR OUTPUT AMPLIFIER CIRCUIT

FIG. 20
PULSE TRANSFORMER TEST CIRCUITS
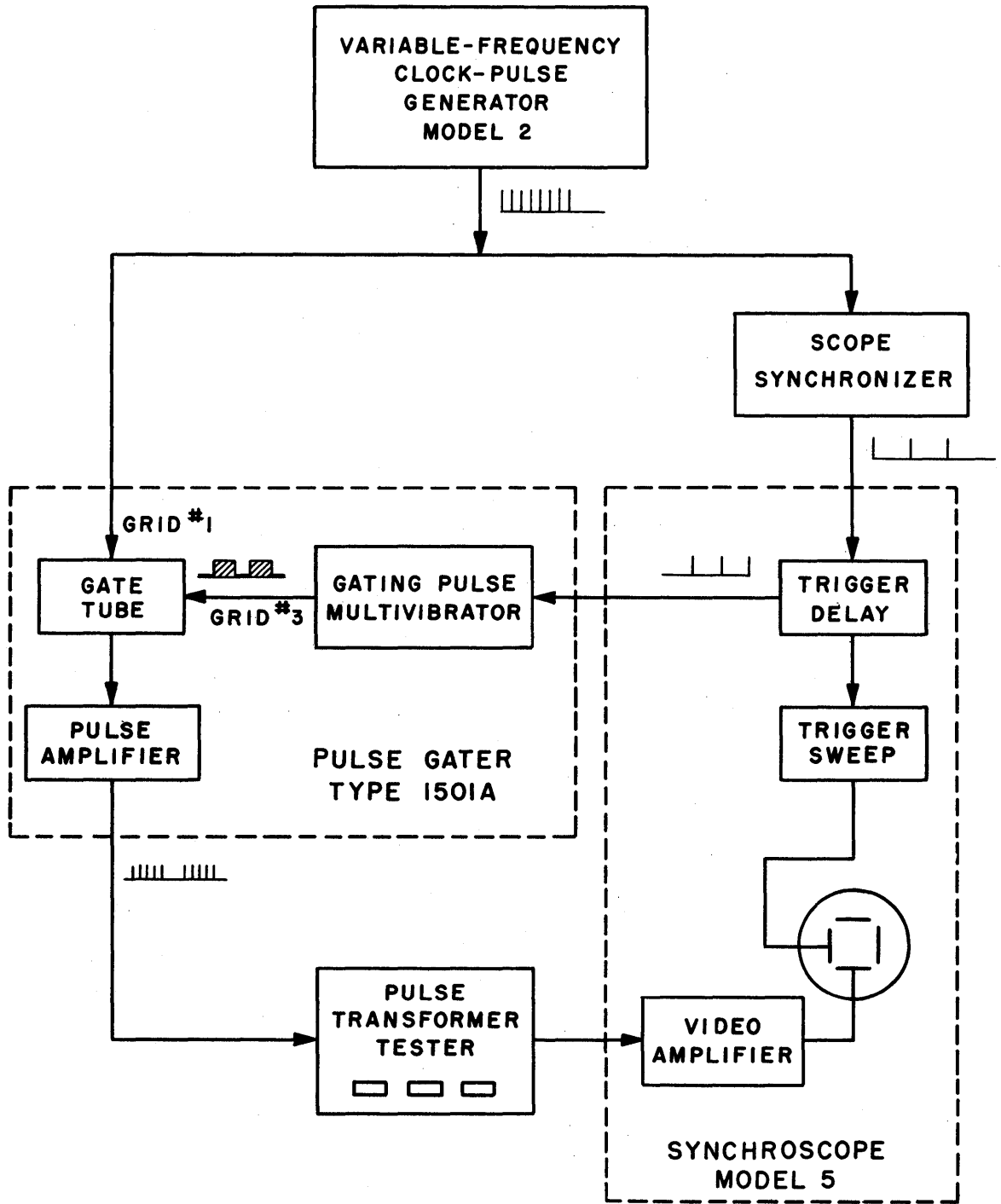
FIG. 21

PULSE GENERATION FOR PULSE
TRANSFORMER TEST

A-52007
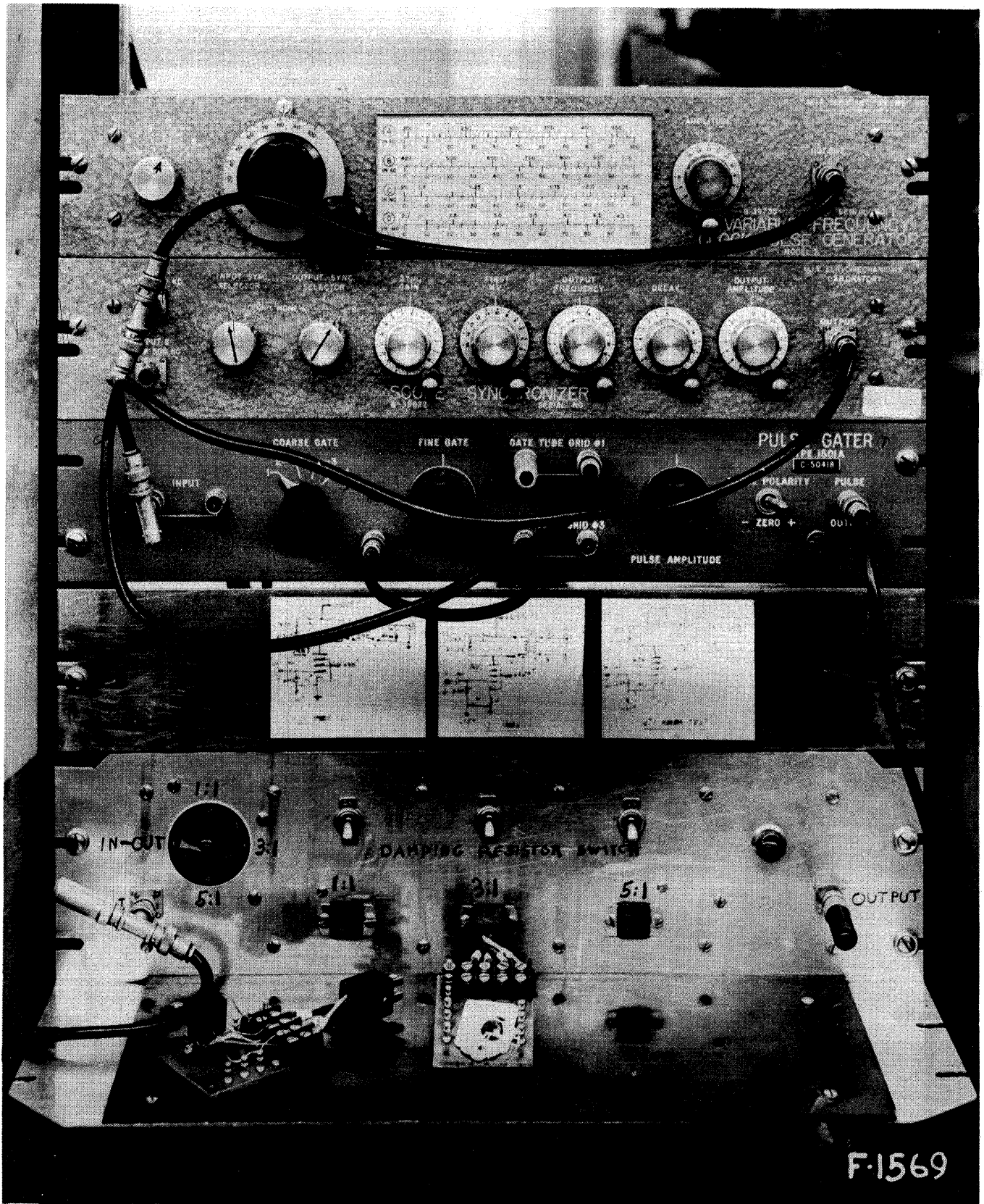
FIG. 22

PULSE TRANSFORMER TEST PANEL
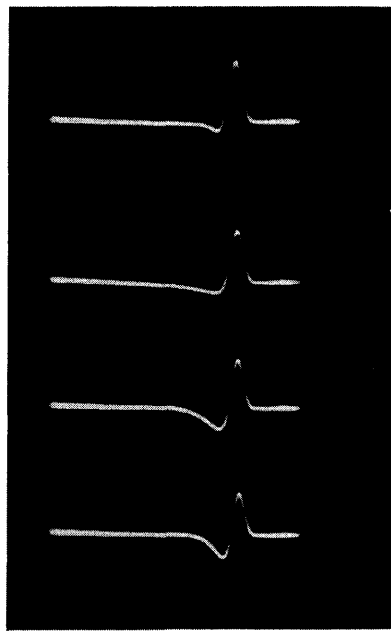
WWI
STANDARD

FERRAMIC H
24:7

FERRICORE
24:7

MFII3I
24:7
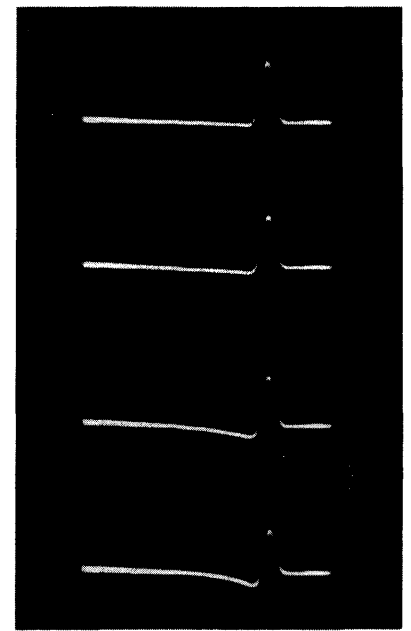
93 Ω LOAD

93 Ω LOAD, DAMPING DIODE
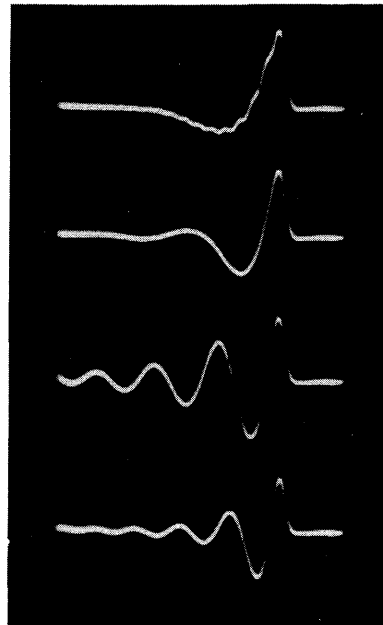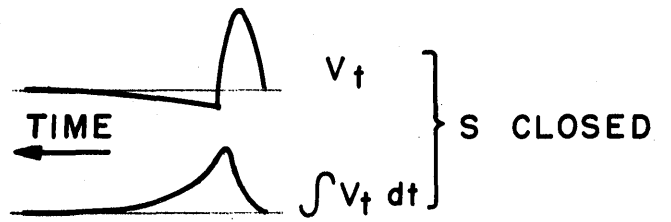
WWI

FERRAMIC H

FERRICORE

MFII3I

OPEN CIRCUIT

FIG. 23

COMPARISON OF 3:I PULSE TRANSFORMER
WITH DIFFERENT CORE MATERIALS

I MIL HYPERSIL

FERRAMIC H

V_t

TIME

$\int V_t \, dt$ ⎫ S CLOSED

V_t

$\int V_t \, dt$ ⎫ S OPEN

FERRICORE

+B

S

3:1

R_d

R
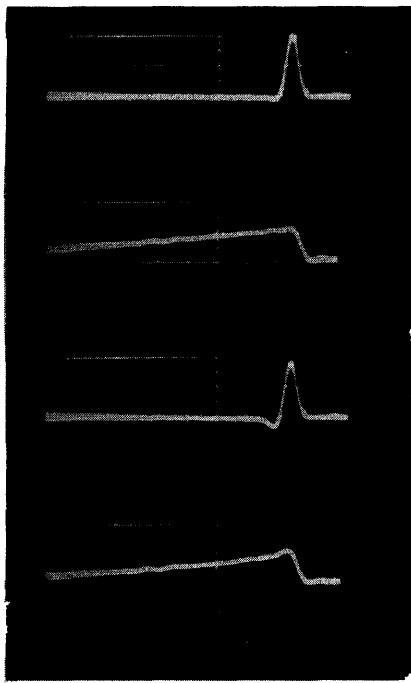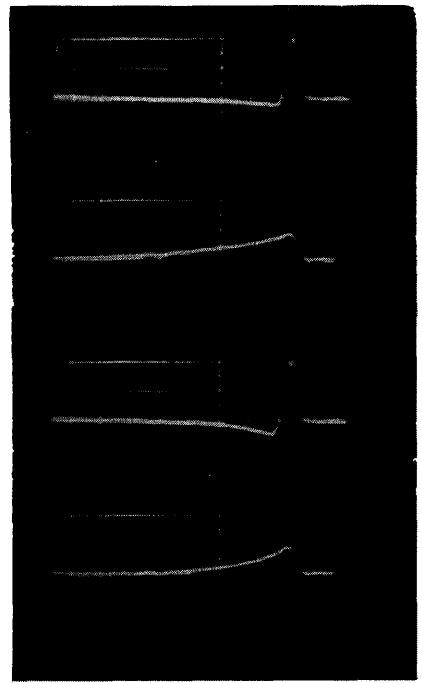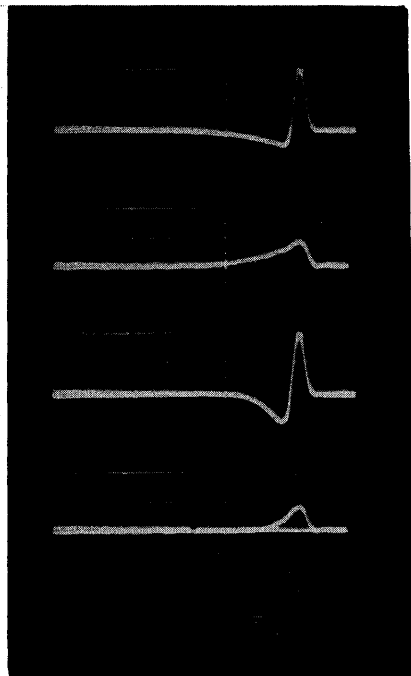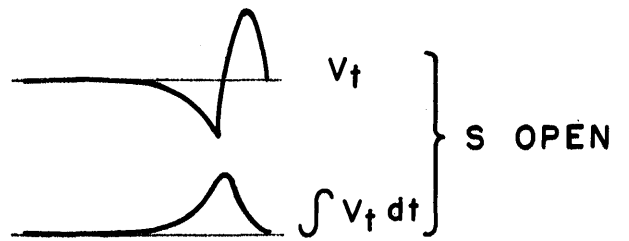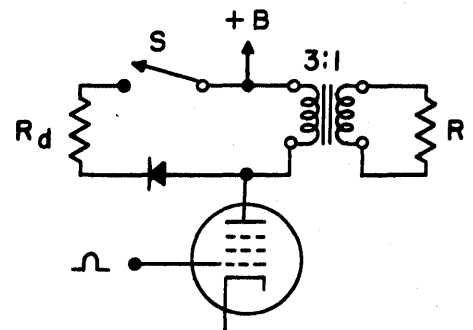
FIG. 24
3:1 PULSE TRANSFORMERS
WITH & WITHOUT DAMPING DIODE
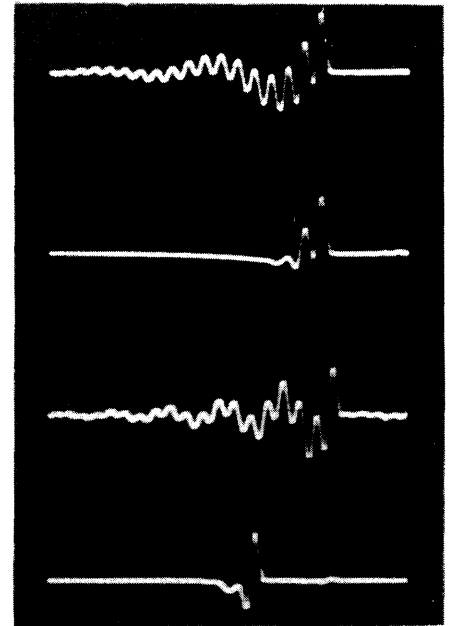
NO DAMPING DIODE
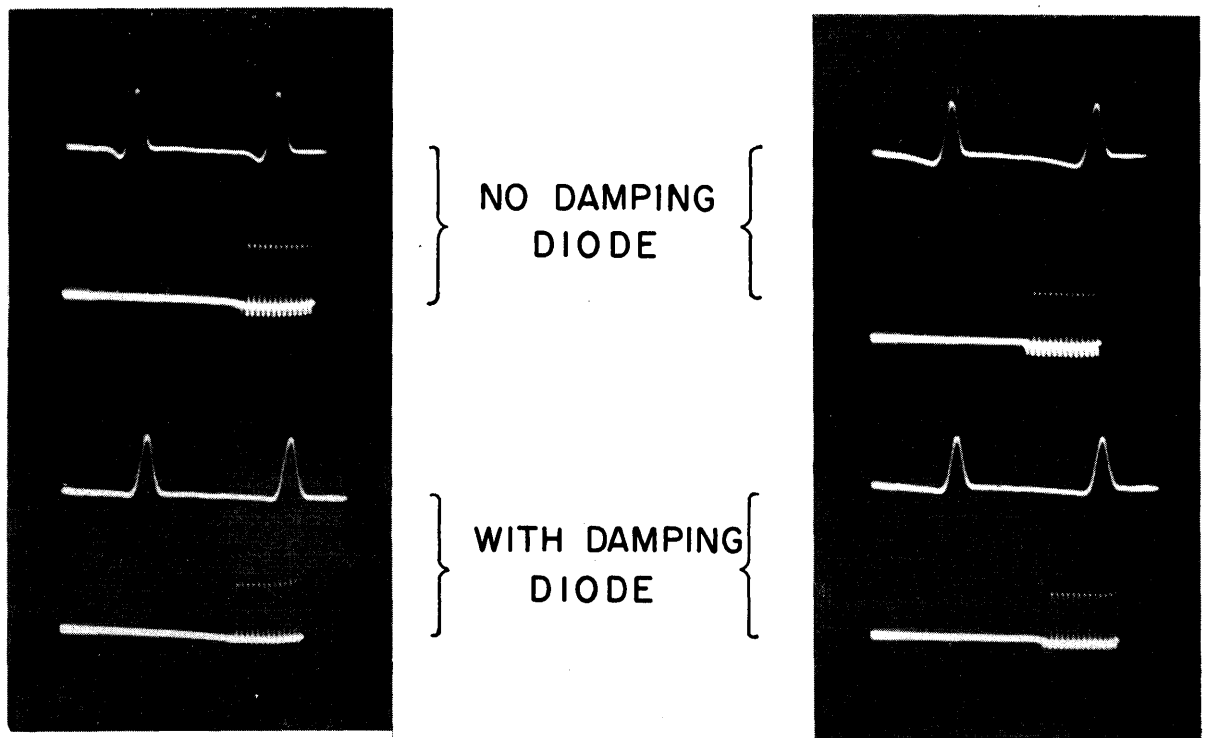
WITH DAMPING DIODE

HYPERSIL

(3:1) TRANSFORMER

FERRAMIC H

(3:1) TRANSFORMER

FIG. 25

EFFECT OF DAMPING DIODE ON

PRF SENSITIVITY
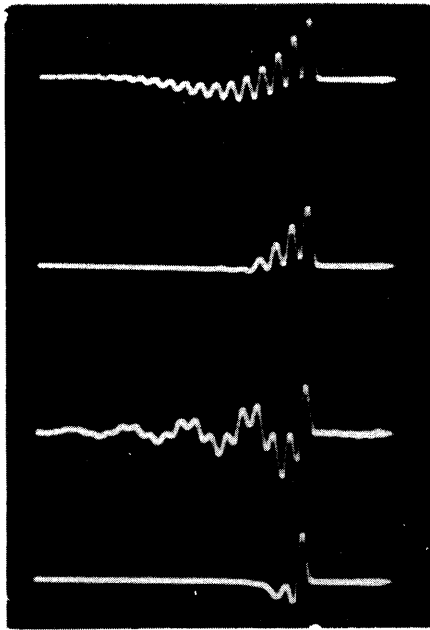
S₁ & S
OPEN

S₁ OPEN
S CLOSED

S OPEN
S₁ CLOSED
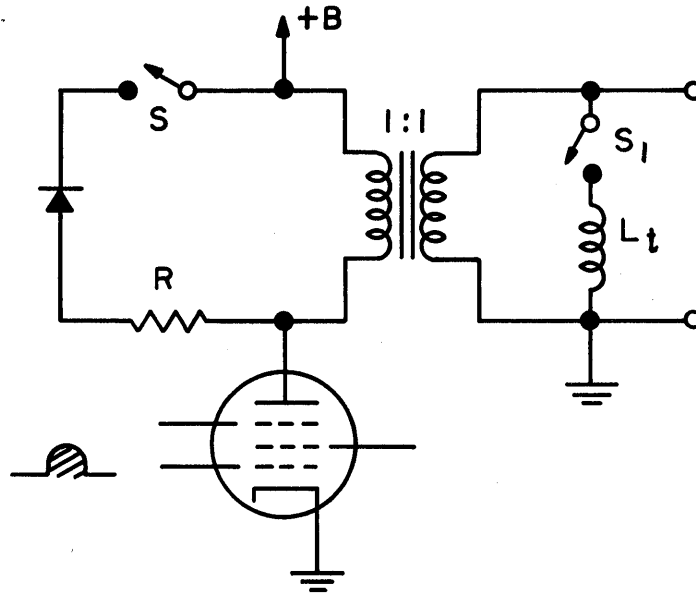
S₁ & S
CLOSED

WWI STANDARD

FERRAMIC H [24:24]

FIG. 26

USE OF TAIL REVERSING INDUCTANCE
IN 1:1 PULSE TRANSFORMERS